Mycosphere 14(1): 777–814 (2023) www.mycosphere.org ISSN 2077 7019
Article
Doi 10.5943/mycosphere/14/1/10

New insights into the classification and evolution of *Favolaschia* (Agaricales, Basidiomycota) and its potential distribution, with descriptions of eight new species

Zhang QY[1], Liu HG[2], Papp V[3], Zhou M[1], Dai YC[1*], and Yuan Y[1*]

[1]*Institute of Microbiology, School of Ecology and Nature Conservation, Beijing Forestry University, Beijing 100083, China*
[2]*Yunnan Key Laboratory of Gastrodia and Fungi Symbiotic Biology, Zhaotong University, Zhaotong 657000, Yunnan China*
[3]*Department of Botany, Hungarian University of Agriculture and Life Sciences, Budapest, Hungary*

Zhang QY, Liu HG, Papp V, Zhou M, Dai YC, Yuan Y 2023 – New insights into the classification and evolution of *Favolaschia* (Agaricales, Basidiomycota) and its potential distribution, with descriptions of eight new species. Mycosphere 14(1), 777–814, Doi 10.5943/mycosphere/14/1/10

Abstract

Favolaschia is a genus of poroid fungi in the order Agaricales with a worldwide distribution. Most studies of *Favolaschia* so far have characterized samples from South America and little information is available on samples from other areas. In this study, species diversity, phylogenetic relationships, divergence time, potential geographic distribution, and the environmental factors that determine the distribution of *Favolaschia* are investigated using a large number of samples covering a wide geographic range in China. Additionally, eight species, viz., *Favolaschia bannaensis*, *F. crassipora*, *F. flabelliformis*, *F. rigida*, *F. semicircularis*, *F. subpustulosa*, *F. tenuissima*, and *F. tephroleuca*, are described as new species based on morphology and molecular phylogenetic analyses inferred from a multi-gene dataset (ITS + nLSU + mtSSU + nuSSU + *tef*1). Morphological descriptions, field photographs, and an identification key are provided. Molecular clock analyses suggest that the common ancestor of *Favolaschia* originated in East Asia, and South and Central America and emerged in the Paleogene period with full support and a mean crown age of 32.0 Mya (95% highest posterior density of 24.9–41.7 Mya), with most species occurring in the Neogene period. The maximum entropy model (Maxent) is applied here to map the potential distribution of *Favolaschia* in the present and in the future, i.e., the 2050s, under four different climate change scenarios in China. The resulting model shows that the precipitation of the warmest quarter has the most important impact on the potential distribution of *Favolaschia* species. The suitability distribution areas of *Favolaschia* species markedly change in the 2050s under different climate change scenarios. Compared to current conditions, the extent of suitable areas for *Favolaschia* species in China are expected to increase in the future with lower greenhouse gas emissions.

Keywords – 8 new taxa – Evolution – Maxent – Phylogeny – Taxonomy – Wood-decaying fungi

Introduction

Favolaschia (Pat.) Pat. was established by Patouillard based on *F. gaillardia* (Pat.) Pat. (Patouillard & Lagerheim 1892), a species formerly described in *Laschia* Fr. (= *Campanella*

Submitted 13 January 2023, Accepted 26 May 2023, Published 20 June 2023
Corresponding Author: Yu-Cheng Dai – e-mail – yuchengdai@bjfu.edu.cn,
Yuan Yuan – e-mail – yuanyuan1018@bjfu.edu.cn

Henn.). The genus is characterized by gelatinous basidiocarps, poroid hymenophore, the presence of gloeocystidia and acanthocystidia which are terminal, mostly swollen tips of hyphae covered by outgrowths (Clémençon 1977), as well as amyloid basidiospores (Patouillard 1900, Singer 1945, 1974, Gillen et al. 2012). *Favolaschia* species prefer hot and humid climates, and usually produce fruiting bodies during the summer and rainy period. The genus has a worldwide distribution and is mainly distributed in tropical to subtropical areas, with a high diversity in South America (Yosio 1952, Singer 1974, Gillen et al. 2012, Magnago et al. 2013).

As mentioned by Singer (1974) and Johnston et al. (2006), *Favolaschia* has a long and complex taxonomic history. The name "*Favolaschia*" was first introduced by Patouillard (1887) as a section of *Laschia*, and later it was treated at generic level (Patouillard & Lagerheim 1892). As of 31 May 2023, there were 119 records of *Favolaschia* recorded in Index Fungorum (http://www.indexfungorum.org), and 134 records in MycoBank (https://www.mycobank.org/), although it is suspected that these taxa represent only around 50 species in the genus (Singer 1974, Parmasto 1999, Kirk et al. 2008). To date, eight *Favolaschia* species have been confirmed in China based on morphology or molecular evidence, viz., *F. brevibasidiata* Q.Y. Zhang and Y.C. Dai, *F. brevistipitata* Q.Y. Zhang and Y.C. Dai, *F. longistipitata* Q.Y. Zhang and Y.C. Dai, *F. minutissima* Q.Y. Zhang and Y.C. Dai, *F. manipularis* (Berk.) Teng, *F. peziziformis* (Berk. and M.A. Curtis) Kuntze, *F. pustulosa* (Jungh.) Kuntze, and *F. tonkinensis* (Pat.) Kuntze; the first four species belong to the *F. calocera* complex (Liu & Yang 1994, Liu 2020, Zhang & Dai 2021).

Previous studies of the genus were mainly based on morphology and phylogenetic studies inferred from sequences of the internal transcribed spacer (ITS) or nuclear large subunit rDNA (nLSU) (Singer 1974, Johnston et al. 2006, Gillen et al. 2012). Recently, molecular biogeography studies have provided important insights into the histories of "species" range changes (Hosaka et al. 2008, Skrede et al. 2011), and several studies have focused on fungal biogeographic distribution and geological events (Floudas et al. 2012, Cai et al. 2014, Chen et al. 2015, Song & Cui 2017). However, the estimation of divergence time and biogeography of *Favolaschia* are unknown so far.

In addition, the ability to identify the spatial distribution of poorly known fungal species is crucial for understanding the environmental factors that affect them and for biological diversity. Ecological niche modelling is a useful tool to assess the potential geographical distribution of species and has been applied to the fields of ecology, biogeography, and evolution (Ganeshaiah et al. 2003, Elith et al. 2006, Peterson et al. 2007). Meanwhile, the geographical distribution of many species may change as a result of climate change in the future. To better understand how climate change affects the distribution of species, the Intergovernmental Panel on Climate Change (IPCC) has simulated future climate change conditions using various models under four different emission scenarios.

A large number of statistical models are currently in use to simulate the spatial distribution of species, and spatial patterns of species diversity (Graham et al. 2006, Sunil & Thomas 2009, Adhikari et al. 2012). The maximum entropy (Maxent) model is a general model for predicting the potential distribution of species, based on the species presence (or occurrence) data and environmental information (Phillips et al. 2004), and has many advantages over other models, including good performance with incomplete datasets, easy operation, small sample size requirements and high simulation precision (Hernandez et al. 2006, Pearson 2007, Ortega-Huerta & Peterson 2008).

In the current study, a phylogenetic analysis of *Favolaschia* was carried out based on a combined sequence dataset of rDNA gene regions [internal transcribed spacer regions (ITS), nuclear large subunit rDNA (nLSU) and small subunit of nuclear ribosomal RNA gene (nuSSU)] and protein-coding regions [small subunit mitochondrial rRNA gene (mtSSU) and translation elongation factor 1a (*tef*1)]. Combined with morphological characters and molecular evidence, eight new species are confirmed to be members of the genus. Currently, 16 species of *Favolaschia* occur in China. Meanwhile, according to the molecular clock analyses based on a dataset (ITS + nLSU + *tef*1), a hypothesis for species diversification and origin of *Favolaschia* is proposed, namely, species of this genus seem to have a polyphyletic origin in East Asia, and South and

Central America. In addition, based on species presence data and environmental information in China, the potential distribution ranges of *Favolaschia* in the present and the future, i.e., the 2050s under different climate change scenarios, are provided by using Maxent.

Materials & Methods

Morphological studies

The studied specimens were deposited in the herbarium of the Institute of Microbiology, Beijing Forestry University (BJFC). Color terms follow Kornerup & Wanscher (1978). Microstructures (including basidiospores) were measured and drawn from dried tissue mounted in Cotton Blue to test for any cyanophilous reaction and Melzer's reagent to text for any amyloid or dextrinoid reaction (following Wu et al. 2022) using a Nikon Eclipse 80i microscope (Tokyo, Japan). The following abbreviations are used: KOH = 5% potassium hydroxide; IKI = Melzer's reagent, IKI+ = amyloid; CB = Cotton Blue, CB– = acyanophilous in Cotton Blue; L = arithmetic average of basidiospores length, W = arithmetic average of basidiospores width, Q = L/W ratios, (*n* = x/y) = the number of spores (x) measured from a given number of specimens (y).

Molecular studies and phylogenetic analysis

A cetyl trimethylammonium bromide (CTAB) rapid plant genome extraction kit (Aidlab Biotechnologies, Co., Ltd., Beijing, China) was used to extract DNA (Wu et al. 2020). The primer pairs of ITS, nLSU, mtSSU, nuSSU, and *tef*1, for amplifying the DNA regions are mentioned in Table 1.

Table 1 PCR primers used in this study.

Gene	Primer	Primer sequences (5′–3′)	References
ITS	ITS5	GGA AGT AAA AGT CGT AAC AAG G	White et al. (1990)
	ITS4	TCC TCC GCT TAT TGATAT GC	White et al. (1990)
nLSU	LR0R	ACC CGC TGA ACT TAA GC	Vilgalys & Hester (1990)
	LR7	TAC TAC CAC CAA GAT CT	Vilgalys & Hester (1990)
mtSSU	MS1	CAG CAG TCA AGA ATA TTA GTC AAT G	White et al. (1990)
	MS2	GCG GAT TAT CGA ATT AAA TAA C	White et al. (1990)
nuSSU	NS1	GTA GTC ATA TGC TTG TCT C	White et al. (1990)
	NS4	CTT CCG TCA ATT CCT TTA AG	White et al. (1990)
*tef*1	tef-983F	GCY CCY GGH CAY CGT CAY TTY AT	Rehner & Buckley (2005)
	tef-1567R	ACH GTR CCR ATA CCA CCS ATC TT	Rehner & Buckley (2005)

The PCR cycling schedules for different DNA sequences of ITS, nLSU, mtSSU, nuSSU and *tef*1 genes used in this study followed Zhang & Dai (2021). The PCR products were purified and sequenced at the Beijing Genomics Institute (BGI), China with the same primers. All newly generated sequences have been submitted to GenBank and are listed in Table 2. Sequences were aligned with additional sequences downloaded from GenBank (Table 2) using BioEdit (Hall 1999) and Clustal X (Thompson et al. 1997). Sequences of *Mycena seminau* A.L.C. Chew and Desjardin were used as the outgroup after Chew et al. (2014).

Maximum Likelihood (ML) and Bayesian Inference (BI) were used to perform phylogenetic analysis of the aligned dataset. RAxML 7.2.8 was used to construct ML trees for both datasets with the GTR+I+G model of site substitution, including estimation of Gamma-distributed rate heterogeneity and a proportion of invariant sites (Stamatakis 2006). The branch support was evaluated with a bootstrapping method of 1000 replicates (Hillis & Bull 1993).

The BI was conducted with MrBayes 3.2.6 in two independent runs, each of which had four chains for 5 million generations and started from random trees (Ronquist & Huelsenbeck 2003). Trees were sampled every 1000th generation. The first 25% of the sampled trees were discarded as

burn-in and the remaining ones were used to reconstruct a majority rule consensus and calculate Bayesian Posterior Probabilities (BPP) of the clades.

Phylogenetic trees were visualized using Treeview (Page 1996). Branches that received bootstrap support for ML (≥75%) and BPP (≥0.95) were considered as significantly supported.

Table 2 Taxa information and GenBank accession numbers of sequences used in this study.

Species	Specimen No.	Locality	ITS	nLSU	mtSSU	nuSSU	*tef1*
Amylocorticium cebennense	HHB-2808	USA	GU187505	GU187561	–	–	GU187675
Anomoloma flavissimum	Cui 12188	China	KT954956	KT954970	–	–	–
Athelia arachnoidea	CBS:418.72	Netherlands	GU187504	GU187557	–	–	GU187672
Auricularia heimuer	Xiaoheimao	–	LT716074	KY418890	–	–	KY419083
Bondarzewia mesenterica	DD 348/06	–	KM243328	KM243331	–	–	KX066147
Calocera cornea	AFTOL438	USA	AY789083	AY701526	–	–	AY881019
Campanella alba	TFB12565	USA	DQ449943	–	–	–	–
Campanella alba	TENN-F-060782	USA	–	MK277678	–	–	–
Clavaria zollingeri	3502	–	KM248911	–	–	–	–
Clavaria zollingeri	MA53142	Norway	–	JQ415955	–	–	–
Clavaria zollingeri	TENN 58652	USA	–	–	–	–	AY881024
Coltricia perennis	Cui 10319	China	KU360687	KU360653	–	–	KY693935
Cruentomycena allochra	HMJAU48195	China	MW222649	MW222660	–	–	–
Dacryopinax spathularia	AFTOL 454	USA	AY854070	AY701525	–	–	AY881020
Echinodontium tinctorium	B1122	–	AF218397	–	–	–	–
Echinodontium tinctorium	AFTOL455	USA	–	–	–	–	AY885157
Favolaschia andina	KG0025	Panama	HM246678	HM246679	–	–	–
F. aurantiaca	FK2047	Brazil	JX987670	–	–	–	–
F. aurantiaca	KG0013	Panama	–	HM246676	–	–	–
F. auriscalpium	Isolate 5	–	KY649461	–	–	–	–
F. auriscalpium	TH1018	Guyana	DQ026241	–	–	–	–
F. austrocyatheae	PDD75609	New Zealand	NR132809	–	–	–	–
F. austrocyatheae	PDD75609	New Zealand	DQ026257	–	–	–	–
F. bannaensis	**Dai 22587**	**Yunnan, China**	**ON870497**	**ON870473**	–	**ON870528**	–
F. bannaensis	**Dai 22589**	**Yunnan, China**	**ON870498**	**ON870474**	–	**ON870529**	–
F. bannaensis	**Dai 22590**	**Yunnan, China**	**ON870499**	**ON870475**	**ON870461**	**ON870530**	–
F. brevibasidiata	Cui 6573	Hainan, China	MZ661794	–	MZ661749	MZ661765	MZ959379
F. brevibasidiata	JM98186	Yunnan, China	DQ026239	–	–	–	–
F. brevistipitata	Dai 19780	Yunnan, China	MZ661772	MZ661742	MZ661753	MZ661769	MZ959383
F. brevistipitata	Dai 19855	Yunnan, China	MZ661773	MZ661743	MZ661754	MZ661770	MZ959384
F. brevistipitata	Dai 19856	Yunnan, China	MZ661774	MZ661744	MZ661755	MZ661771	MZ959385
F. calocera	PC99060	Madagascar	DQ26252	–	–	–	–
F. calocera	PC99497	Madagascar	DQ026253	–	–	–	–
F. cinnabarina	4421	Brazil	JX987669	–	–	–	–
F. cinnabarina	DUKE4039	Puerto Rico	DQ026242	–	–	–	–

Table 2 Continued.

Species	Specimen No.	Locality	ITS	nLSU	mtSSU	nuSSU	*tef1*
F. cinnabarina	RVPR82	–	–	AF261416	–	–	–
F. claudopus	Dai 18656	Australia	MZ661775	MZ661735	MZ661745	MZ661761	–
F. claudopus	Dai 18663	Australia	MZ661776	MZ661734	–		MZ959375
F. claudopus	SR346	Kenya	DQ026237	–	–	–	–
F. claudopus	PDD74554	New Zealand	DQ026251	–	–	–	–
F. claudopus	PDD75323	New Zealand	DQ026248	–	–	–	–
F. claudopus	PDD75686	New Zealand	DQ026249	–	–	–	–
F. claudopus	DUKE2952	New Zealand	DQ026238	–	–	–	–
F. crassipora	**Dai 19769**	**Yunnan, China**	**ON870500**	**ON870476**	**ON870462**	**ON870531**	–
F. crassipora	**Dai 19871**	**Yunnan, China**	**ON870501**	**ON870477**	–	**ON870532**	–
F. cyatheae	PDD75316	New Zealand	NR132808	–	–	–	–
F. cyatheae	PDD75316	New Zealand	DQ026256	–	–	–	–
F. dealbata	KG0015	Panama	–	HM246677	–	–	–
F. flabelliformis	**Dai 20010**	**Yunnan, China**	**ON870502**	**ON870478**	–	**ON870533**	–
F. flabelliformis	**Dai 20016**	**Yunnan, China**	**ON870503**	–	–	**ON870534**	–
F. heliconiae	KG0026	Panama	–	HM246680	–	–	–
F. longistipitata	Dai 13221	Yunnan, China	MZ661777	–	–	–	–
F. longistipitata	Dai 13226	Yunnan, China	MZ661778	–	–	–	–
F. longistipitata	Cui 11128	Yunnan, China	MZ661779	–	–	–	–
F. longistipitata	Dai 17597	Yunnan, China	MZ661780	–	–	–	–
F. longistipitata	Dai 17598	Yunnan, China	MZ661781	–	–	–	–
F. longistipitata	Dai 17601	Yunnan, China	MZ661782	–	–	–	–
F. longistipitata	Dai 19799	Yunnan, China	MZ661784	MZ661739	MZ661750	MZ661766	MZ959380
F. longistipitata	Dai 19893	Yunnan, China	MZ661785	MZ661740	MZ661751	MZ661767	MZ959381
F. longistipitata	Dai 20019	Yunnan, China	MZ661786	MZ661741	MZ661752	MZ661768	MZ959382
F. longistipitata	Dai 20328	Yunnan, China	MZ661787	–	–	–	–
F. longistipitata	Dai 20341	Yunnan, China	MZ661788	–	–	–	–
F. longistipitata	Dai 20355	Yunnan, China	MZ661789	–	–	–	–
F. luteoaurantiaca	4475	–	JX987667	–	–	–	–
F. luteoaurantiaca	SP445750	Brazil	NR132874	–	–	–	–
F. macropora	KG0027	Panama	NR132845	HM246682	–	–	–
F. manipularis	Dai 20612	Yunnan, China	MZ801776	MZ914395	–	–	–
F. manipularis	Dai 20653	Yunnan, China	MZ801777	–	–	–	–
F. minutissima	JM98372	Thailand	DQ026240	–	–	–	–

Table 2 Continued.

Species	Specimen No.	Locality	ITS	nLSU	mtSSU	nuSSU	*tef1*
F. minutissima	Dai 10753	Hainan, China	MZ661790	–	–	–	–
F. minutissima	Dai 20085	Hainan, China	MZ661791	MZ661736	MZ661746	MZ661762	MZ959376
F. minutissima	Dai 20086	Hainan, China	MZ661792	MZ661737	MZ661748	MZ661764	MZ959378
F. minutissima	Dai 20088	Hainan, China	MZ661793	MZ661738	MZ661747	MZ661763	MZ959377
F. peziziformis	ICMP1575	Japan	DQ026255	–	–	–	–
F. peziziformis	PDD67440	New Zealand	–	AY572008	–	–	–
F. pustulosa	DUKE3316	Papua New Guinea	DQ026245	–	–	–	–
F. pustulosa	PDD75686	New Zealand	DQ026254	–	–	–	–
F. pustulosa	Dai 19758	Yunnan, China	MT292325	MT293226	–	–	–
F. pustulosa	Dai 19892	Yunnan, China	MT292326	MT293227	–	–	–
F. rigida	**Dai 18566A**	**Guangxi, China**	**ON870504**	**ON870479**	**ON870463**	–	–
F. rigida	**Dai 20764**	**Yunnan, China**	**ON870505**	**ON870480**	–	**ON870535**	–
F. rigida	**Dai 22614**	**Fujian, China**	**ON870506**	–	–	**ON870536**	–
F. semicircularis	**Dai 19725**	**Guangdong, China**	**ON870507**	**ON870481**	**ON870464**	**ON870537**	**OP331313**
F. semicircularis	**Dai 19923**	**Yunnan, China**	**ON870508**	**ON870482**	–	**ON870538**	–
F. semicircularis	**Dai 19936**	**Yunnan, China**	**ON870509**	**ON870483**	–	**ON870539**	–
F. semicircularis	**Dai 19939**	**Yunnan, China**	**ON870510**	–	–	**ON870540**	–
F. semicircularis	**Dai 19980**	**Yunnan, China**	**ON870511**	**ON870484**	**ON870465**	**ON870541**	–
F. semicircularis	**Dai 19981**	**Yunnan, China**	**ON870512**	**ON870485**	**ON870466**	**ON870542**	–
F. semicircularis	**Dai 22290**	**Zhejiang, China**	**ON870513**	**ON870486**	–	**ON870543**	**OP331314**
F. semicircularis	**Dai 22291**	**Zhejiang, China**	**ON870514**	**ON870487**	**ON870467**	**ON870544**	–
F. semicircularis	**Dai 22298**	**Zhejiang, China**	**ON870515**	**ON870488**	–	**ON870545**	**OP331315**
F. semicircularis	**Dai 22302**	**Zhejiang, China**	**ON870516**	–	–	**ON870546**	**OP331316**
F. semicircularis	**Dai 22383**	**Fujian, China**	**ON870517**	–	**ON870468**	**ON870547**	–
Favolaschia sp. 1	DUKE2708	Australia	DQ026234	–	–	–	–
Favolaschia sp. 1	DUKE2876	Australia	DQ026235	–	–	–	–
Favolaschia sp. 1	DUKE3195	Papua New Guinea	DQ026236	–	–	–	–
Favolaschia sp. 2	4550	Panama	JX987668	–	–	–	–
F. sprucei	TH6418	Guyana	DQ026246	–	–	–	–
F. subpustulosa	**Dai 20719**	**Yunnan, China**	**ON870518**	**ON870489**	**ON870469**	**ON870548**	**OP331317**
F. tenuissima	**Dai 22071**	**Hainan, China**	**ON870519**	**ON870490**	**ON870470**	**ON870549**	–
F. tenuissima	**Dai 22072**	**Hainan, China**	**ON870520**	**ON870491**	–	**ON870550**	–

Table 2 Continued.

Species	Specimen No.	Locality	ITS	nLSU	mtSSU	nuSSU	*tef1*
F. tephroleuca	**Dai 22282**	**Yunnan, China**	**ON870521**	**ON870492**	**ON870471**	**ON870551**	–
F. tephroleuca	**Dai 22288**	**Chongqing, China**	**ON870522**	**ON870493**	**ON870472**	**ON870552**	–
F. tonkinensis	**Dai 21955**	**Hainan, China**	**ON870523**	**ON870494**	–	–	**OP331318**
F. tonkinensis	**Dai 21956**	**Hainan, China**	**ON870524**	**ON870495**	–	**ON870553**	**OP331319**
F. tonkinensis	**Dai 21964**	**Hainan, China**	**ON870525**	–	–	**ON870554**	**OP331320**
F. tonkinensis	**Dai 21965**	**Hainan, China**	**ON870526**	**ON870496**	–	**ON870555**	**OP331321**
F. tonkinensis	**Dai 21966**	**Hainan, China**	**ON870527**	–	–	**ON870556**	**OP331322**
F. varariotecta	DUKE3893	Puerto Rico	DQ026243	–	–	–	–
F. varariotecta	DUKE4038	Puerto Rico	DQ026244	–	–	–	–
Fomitiporia mediterranea	AFTOL 688	USA	AY854080	AY684157	–	–	AY885149
Gautieria otthii	T7852L	USA	AF377072	AF393058	–	–	AY883434
Gomphidius roseus	CUW	Germany	DQ534570	DQ534669	–	–	–
Gomphidius roseus	MB95-038	Germany	–	–	–	–	GU187702
Gymnopilus picreus	taxon:171472		LT716066	KY418882	–	–	KY419077
Heterobasidion tibeticum	Dai 5534	China	KJ651506	KJ651564	–	–	–
Hygrocybe conica	KUBOT-KRMK-2020-61	India	MW449855	MW449854	–	–	–
Lepiota cristata	taxon:56166	–	LT716026	KY418841	–	–	KY419048
Marasmiellus candidus	CBS:252.39	–	MH856003	MH867503	–	–	–
Marasmius rotula	KUBOT-KRMK-2020-109	India	MW504471	MW504469	–	–	GU187723
Mycena filopes	HMJAU43562	China	MH396635	MK722350	–	–	–
Mycena pura	KUBOT-KRMK-2020-114	India	MW504828	MW504829	–	–	–
Mycena seminau	ACL136	Malaysia	KF537250	KJ206952	–	–	–
Mycena seminau	ACL308	Malaysia	KF537252	KJ406376	–	–	–
Mycena vulgaris	CBS 248.47	France	MH856240	MH867770	–	–	–
Neurospora crassa	OR74A	USA	HQ271348	AF286411	–	–	XM959775
Panellus pusillus	Dai 20434	China	MZ801775	MZ914394	–	–	–
Panellus stypticus	JP 2998	Finland	MT705625	–	–	–	–
Phellinus hartigii	Cui 9914	China	KY750527	KY750528	–	–	KY750529
Ramaria rubella	AFTOL 724	USA	AY854078	AY645057	–	–	AY883435
Resinomycena ellipsoidea	HMJAU48194	China	MW222651	MW222661	–	–	–
Roridomyces roridus	HMJAU47832	China	MW222643	–	–	–	–
Schizosaccharomyces pombe	IFO1608	–	AB054041	JN938920	–	–	–
Stereum hirsutum	CLZhao 7420	China	OM955779	OM946599	–	–	–
Stereum hirsutum	AFTOL492	USA	–	–	–	–	AY885159
Suillus pictus	AFTOL 717	USA	AY854069	AY684154	–	–	AY883429
Vanrija humicola	SJ17	China	FJ515176	FJ515231	–	–	DQ645519

Notes: New sequences are in bold; "–" represents missing data.

Divergence time estimation

In this study, a dataset with 66 specimens was used to infer the divergence times of species in

the genus *Favolaschia* based on a dataset composed of ITS + nLSU+ *tef1* sequences (Table 2). The BEAST 2.6.5 software package was used to estimate divergence times (Bouckaert et al. 2014). An XML (Extensible Markup Language) file was generated with BEAUti (version 2). The rates of evolutionary changes at nuclear acids were estimated using ModelTest (version 3.7) with the GTR substitution model (Posada & Crandall 1998). Divergence time and corresponding CIs were conducted with a log-normal relaxed molecular clock and the Yule speciation prior. Three fossil time points, i.e., *Archaeomarasmius leggettii* Hibbett et al. (1995, 1997), *Quatsinoporites cranhamii* S.Y. Smith et al. (2004) and Berbee & Taylor (2010), and *Paleopyrenomycites devonicus* Taylor et al. (1999, 2005), representing the divergence time at Agaricales, Hymenochaetaceae, and between Ascomycota and Basidiomycota, respectively, were selected for calibration. The offset age with a gamma distributed prior (scale = 20 and shape = 1) was set as 90, 125, and 400 Mya for Agaricales, Hymenochaetaceae, and Basidiomycota, respectively. After 10,000,000 generations, the first 10% were removed as burn-in. The log file was checked for convergence with Tracer (version 1.54). Consequently, a Maximum Clade Credibility (MCC) tree was summarized with TreeAnnotator (version 2.6.5), annotating clades with more than 0.8 posterior probability (PP).

Inferring historical biogeography

Reconstruct Ancestral State in Phylogenies (RASP) (version 4.2) was used to reconstruct historical biogeography for *Favolaschia* with a dispersal-extinction-cladogenesis (DEC) model (Yu et al. 2015, 2020). Dispersal probabilities between areas are important for the reconstruction when using LAGRANGE (Ree & Smith 2008). The geographic distributions for *Favolaschia* were identified in five areas: (A) East Asia, (B) Europe, (C) Oceania, (D) Africa, (E) South America, (F) Central America, (G) North America.

Species occurrence data and environmental factors

165 records of *Favolaschia* species in China were collected from field survey recording sites deposited in BJFC, online database of the Global Biodiversity Information Facility (GBIF, http://www.gbif.org), and the literature (Liu & Yang 1994, Li et al. 1998, Liu 2020). When the available records lacked specific geo-coordinates, Google Earth 7.0 was utilized to confirm the approximate latitude and longitude, according to the described geographical locations (https://earth.google.com/). Then, duplicate and invalid distribution points were deleted, and finally 84 records from 16 species of *Favolaschia* effective distribution points were determined.

19 bioclimatic variables with 5 arc minutes (ca. 10 km) spatial resolution, were downloaded from WorldClim (www.worldclim.org) database (Table 3). The climate data used to predict the potential geographic distribution of *Favolaschia* species under climate change scenarios included the baseline climate condition data [time period: current (average for 1970–2000)] and the climate scenario data [time periods: 2050s (average for 2041–2060)]. Modeling data was from the Beijing Climate Center–Climate System Model (BCC-CSM 1.1). The sixth IPCC assessment report published four shared socio-economic pathways (SSPs), 126, 245, 370 and 585, that represents greenhouse gas emissions globally from lowest to highest (Zhang et al. 2019, Jiang et al. 2020).

Table 3 Environmental variables used to create the species distribution model and their percentage contribution to model performance.

Abbreviation	Description	Unit	Contribution %
Bio1	Annual mean temperature	℃	–
Bio2	**Mean diurnal range (mean of monthly (max temp - min temp))**	**℃**	1.8
Bio3	**Isothermality (Bio2/Bio7) (× 100)**	**C of V**	0.5
Bio4	**Temperature seasonality (standard deviation × 100)**	**℃**	19.4
Bio5	Maximum temperature of warmest month	℃	–
Bio6	Minimum temperature of coldest month	℃	–

Table 3 Continued.

Abbreviation	Description	Unit	Contribution %
Bio7	Temperature annual range (Bio5–Bio6)	℃	–
Bio8	**Mean temperature of wettest quarter**	**℃**	1.5
Bio9	Mean temperature of driest quarter	℃	–
Bio10	Mean temperature of warmest quarter	℃	–
Bio11	Mean temperature of coldest quarter	℃	–
Bio12	Annual precipitation	mm	–
Bio13	Precipitation of wettest month	mm	–
Bio14	**Precipitation of driest month**	**mm**	5.8
Bio15	Precipitation seasonality (coefficient of variation)	C of V	–
Bio16	Precipitation of wettest quarter	mm	–
Bio17	Precipitation of driest quarter	mm	–
Bio18	**Precipitation of warmest quarter**	**mm**	71
Bio19	Precipitation of coldest quarter	mm	–

Notes: The highlighted variables represent the environmental variables that are ultimately used to predict the potential distribution of *Favolaschia* species.

Maxent analysis

The training data were 75% of the sample data selected randomly, and the test data were the remaining 25% of the sample data. The maximum number of background points was set to 10,000 with the maximum number of iterations fixed at 3000 to ensure the model had adequate time to converge, while the other values were kept at their default levels. Ten replicates were executed to evaluate the averaged results. The habitat suitability curves of each variable were calculated, and the importance of each environmental variable to the habitat model of *Favolaschia* was calculated using the software's built-in jackknife test. The file format was set for logistic output which provides predicted probabilities of presence between 0 and 1.

Many environmental variables are spatially correlated and might lead to the overfitting of the prediction (Li et al. 2020). Therefore, Spearman's correlation coefficients were used to examine the correlation of 19 bioclimatic factors by SPSS 26.0. If the coefficient was less than 0.8, the environmental variable was retained; when two variables had a Spearman's coefficient larger than 0.8, the one with less ecological significance was discarded (Yi et al. 2016, Zhang et al. 2021). Finally, 6 out of 19 environmental variables were selected as environmental variables for the prediction process (Table 3).

The accuracy of each model prediction was quantified by calculating the area under the Receiver Operating Characteristic (ROC) curve (AUC) (Lobo et al. 2008). AUC values range from 0.5 to 1.0, with 0.5 indicating no (random) fit to the data, 1.0 indicating perfect model performance, and values larger than 0.9 indicating high performance (Pearce & Ferrier 2000). The generated potential review maps are beautified by DIVA-GIS 7.5.0. The final potential species distribution map had a range of values from 0 to 1 which were regrouped into five classes of potential habitats, viz., non-suitability area (< 0.02), marginal suitability area (0.02–0.2), low suitability area (0.2–0.4), medium suitability area (0.4–0.6), and high suitability area (> 0.6).

Results

Phylogenetic analyses

The phylogeny of combined five genes (ITS + nLSU + mtSSU + nuSSU + *tef*1) from 93 fungal specimens representing 32 taxa in *Favolaschia* was carried out. The best model estimated and applied in the Bayesian analysis was GTR+I+G. The ML analysis resulted in the best tree (Fig. 1). BI analyses resulted in almost identical tree topologies compared to the ML analysis, with an average standard deviation of split frequencies of 0.006644 (BI). Additionally, only the ML tree is presented along with the support values from the BI analyses.

In our phylogenetic tree, most *Favolaschia* species cluster within two groups (A and B in Fig. 1), which corresponds to the sections proposed by Singer (1974): *Favolaschia* sect. *Favolaschia* (Group A) and *Favolaschia* sect. *Anechinus* (Group B). *Favolaschia manipularis* forms a separate clade. Additionally, the phylogenetic tree (Fig. 1) reveals that eight new and independent lineages represented by our specimens nest in *Favolaschia* sect. *Anechinus* (Group B).

Divergence time estimation for *Favolaschia*

A combination of ITS, nLSU, and *tef1* sequences are used to estimate the divergence time of *Favolaschia*. The MCC in Fig. 2 shows that the Mycenaceae emerged earlier with a mean stem age of 111.1 Mya [95% highest posterior density (HPD) of 102.7–119.7 Mya] and a mean crown age of 74.3 Mya (95% HPD of 56.0–95.3 Mya), which is consistent with previous studies (Chen et al. 2015, Zhu et al. 2019). In Mycenaceae, the initial diversification of *Favolaschia* occurred during the Oligocene (32.0 Mya, 95% HPD of 24.9–41.7 Mya). The divergence of most species in *Favolaschia* occurred mainly during the Neogene period.

The historical biogeography of *Favolaschia*

The inferred historical biogeographic scenarios from the analyses using RASP are shown in Fig. 3. The results of the Dispersal-Extinction-Cladogenesis (DEC) analysis suggest a complex biogeographic history for *Favolaschia*. Twenty-three dispersal events and seven vicariance events are needed to explain the present distribution of the genus. The RASP analysis supports that East Asia, and South and Central America have the highest probability of being the ancestral area of *Favolaschia*. In addition, ancestral species of group I probably arose in South America at about 23.3 Mya, whereas the ancestral species of group II probably emerged in East Asia, around 22.4 Mya, and the ancestral species of group III probably emerged in East Asia and Oceania around 23.7 Mya

Taxonomy

Favolaschia bannaensis Q.Y. Zhang & Y.C. Dai, sp. nov. Figs 4a, 5a, 6

Index Fungorum number: IF900426; Facesoffungi number: FoF14232

Etymology – "*bannaensis*" (Lat.): refers to Xishuangbanna, Yunnan, China where the species was first found.

Basidiocarps annual, gregarious, gelatinous when fresh and dry. *Pilei* 2–5 × 1.5–4 mm, conchoid, semicircular or ellipsoid; pileal surface white (A1) to satin white (2A1) when fresh, yellowish white (1A2–2A2) upon drying, convex, transparent with a reticulate pattern matching the pores below, glabrous; margin straight, crenulate or entire; context thin, transparent. *Hymenophore* concolorous with pileal surface, poroid, about 15–30 pores per basidiocarp; mature pores 0.5–1.5 mm diam., polygonal, larger near the base and smaller near the edge, the marginal pores often incomplete; tubes up to 0.3 mm long. *Stipe* absent.

Basidiospores (7–)7.5–9.2(–10) × 4–6 μm, L = 8.36 μm, W = 5.09 μm, Q = 1.58–1.71 (*n* = 90/3), oblong-ellipsoid, hyaline, thin-walled, smooth, with one or two guttules, faintly IKI+, CB–. *Basidia* 30–38 × 7–10 μm, cylindrical or clavate with some guttules, 2(–4)–spored, sterigmata 3–6 μm long; basidioles similar in shape to the basidia, but slightly smaller. Gloeocystidia and acanthocystidia absent. *Cheilocystidia* 15–25 × 5–12 μm, present at dissepiment edge, broom-shaped, with obtuse diverticulate projections on the sides and at the apex, thin-walled. *Pileipellis* hyphae interwoven, smooth to diverticulate, thin-walled, 3–8 μm diam.; terminal cells in shape similar to cheilocystidia, oriented perpendicular to pileal surface. *Tramal* hyphae interwoven, widely spaced in a gelatinous matrix, some with dense contents, some collapsed, thin-walled, 1.5–4 μm diam. *Clamp connections* present.

Known distribution – Tropical regions of China.

Material examined – CHINA, Yunnan Province, Jinghong, Xishuangbanna Virgin Forest Park, rotten angiosperm wood, 7 Jul 2021, Y. C. Dai, Dai 22585 (BJFC 037159, paratype), Dai

22589 (BJFC 037163, paratype); rotten angiosperm branch, Dai 22587 (BJFC 037161, paratype); on dead bamboo (Bambusoideae), Dai 22590 (BJFC 037164, holotype).

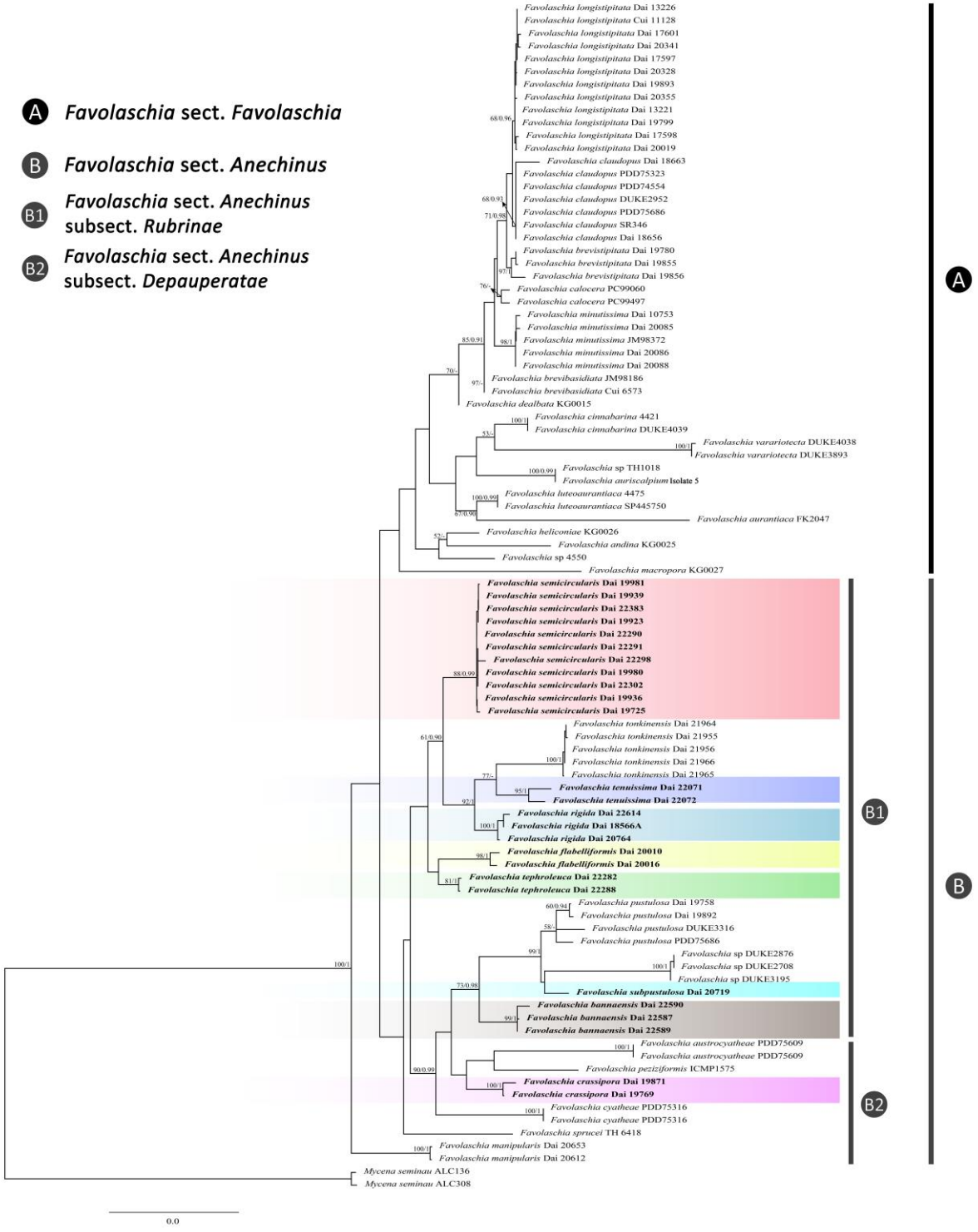

Figure 1 – Maximum Likelihood (ML) tree illustrating the phylogeny of *Favolaschia* based on a combined 5-gene (ITS + nLSU + mtSSU + nuSSU + *tef1*) dataset. Branches are labeled with parsimony bootstrap values (ML) higher than 50%, and Bayesian Posterior Probabilities (BPPs) more than 0.90.

Notes – *Favolaschia bannaensis* was discovered in the tropical area of Yunnan Province of China. Based on the sub-generic classification of *Favolaschia* by Singer (1974), morphologically

F. bannaensis matches *Favolaschia* sect. *Anechinus* subsect. *Rubrinae*, because it lacks acanthocystidia, gloeocystidia and gloeoplerous hyphae. Phylogenetically, the samples of *F. bannaensis* (Dai 22587, Dai 22589 and Dai 22590) formed an independent linage (99% ML, 1 BPP, Fig. 1), and it is related to *F. pustulosa*, *F. subpustulosa* and an undetermined *Favolaschia* species from Australia (*Favolaschia* sp. 1). The sequences of *Favolaschia* sp. 1 specimens (DUKE2708, DUKE2876 and DUKE3105) were retrieved from GenBank. We failed to obtain specimens of the taxon, but it formed an independent lineage with a highly supported subgroup (100% ML, 1.00 BPP, Fig. 1), within the *Favolaschia* sect. *Anechinus* subsect. *Rubrinae* clade, so we treated these samples here as *Favolaschia* sp. 1 temporarily. Morphologically, *F. bannaensis*, *F. pustulosa* and *F. subpustulosa* share pure white to white basidiocarps when fresh. However, *F. pustulosa* differs from *F. bannaensis* by its larger basidiocarps (5–85 mm vs. 2–5 mm), and wider basidiospores (5.5–8 µm vs. 4–6 µm in width, Singer 1974). *Favolaschia subpustulosa* differs from *F. bannaensis* by its larger basidiocarps (10–40 mm vs. 2–5 mm), and shorter basidiospores (6–7.5 µm vs. 7–9.2 µm in length).

In addition, *F. peziziformis*, a species in subsect. *Rubrinae*, may be confused with *F. bannaensis* by their similar basidiospores and strongly diverticulate hyphae in the pileipellis. Singer (1974) summarized descriptions of *F. peziziformis* from three versions, of which two specimens of *F. peziziformis* were from the type locality of Japan, and one specimen was from New Zealand. However, *F. peziziformis* from Japan can be easily distinguished from *F. bannaensis* by its gloeocystidia (Kobayasi 1952, Singer 1974). *Favolaschia peziziformis* from New Zealand can be also easily distinguished from *F. bannaensis* by its larger basidiocarps (up to 10 mm vs. 2–5 mm, Singer 1974).

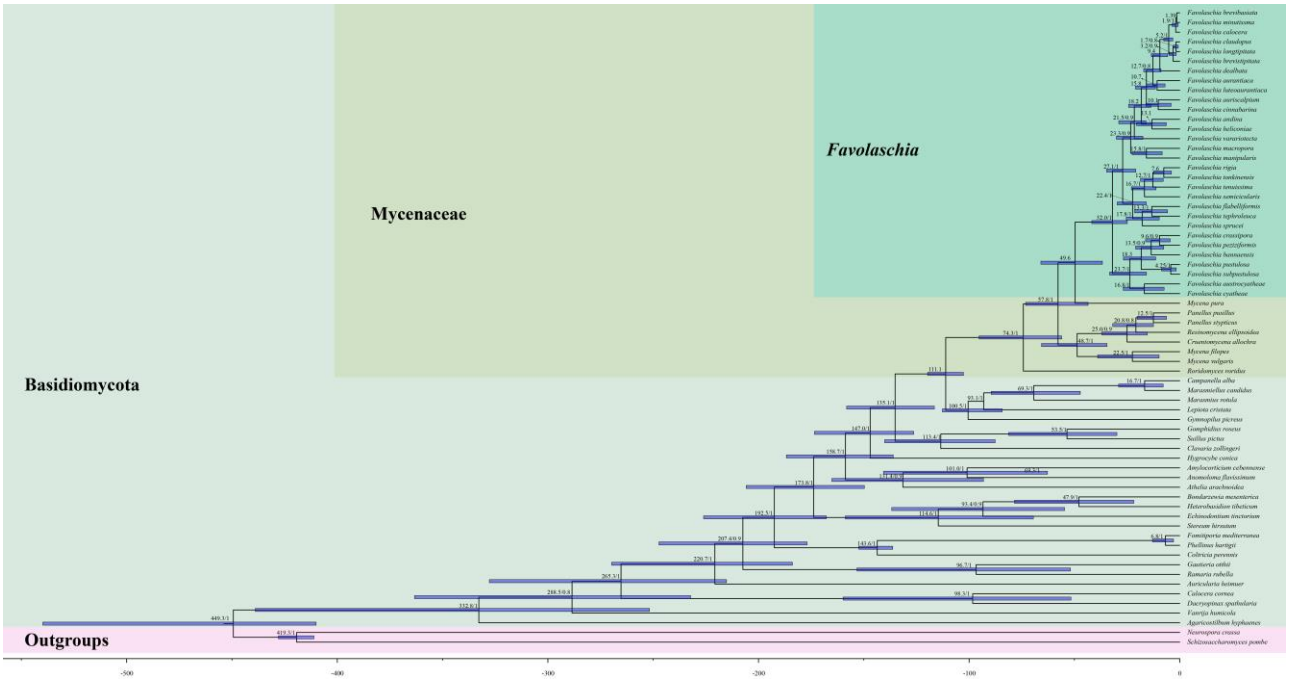

Figure 2 – Estimated divergence of *Favolaschia* generated from molecular clock analyses using a combined dataset of ITS, nLSU and *tef1* sequences. Estimated mean divergence time (Mya) and posterior probabilities (PP) > 0.8 are annotated at the internodes. The 95% highest posterior density (HPD) interval of divergence time estimates are marked by horizontal blue bars.

Favolaschia crassipora Q.Y. Zhang & Y.C. Dai, sp. nov. Figs 4b, 5b, 7

Index Fungorum number: IF 900427; Facesoffungi number: FoF14233

Etymology – "*crassipora*" (Lat.): refers to the pores having thick dissepiments.

Basidiocarps annual, gregarious, gelatinous when fresh and dry. *Pilei* 0.2–2 × 0.2–1.8 mm, semicircular, ellipsoid or circular; pileal surface snow white to white when fresh (A1), pale white

[2A(1–2)] to grayish yellow [4B(3–4)] upon drying, plane to convex, faintly pruinose when dry; margin thick, incurved, entire; context thin, opaque, easily folding or tearing. *Hymenophore* concolorous with pileal surface, poroid, about 15–60 pores per basidiocarp; mature pores 0.12–0.17 mm diam., round with thick dissepiments; tubes up to 0.4 mm long. *Stipe* absent.

Basidiospores 9–13(–13.8) × (6.5–)7–10(–12) µm, L = 11.00 µm, W = 8.63 µm, Q = 1.25–1.31 (*n* = 90/3), broadly ellipsoid to subglobose, hyaline, thin-walled, smooth, with some guttules, faintly IKI+, CB–. *Basidia* 32–41 × 8–12 µm, cylindrical or clavate with some guttules, 2–spored, sterigmata 3–7 µm long; basidioles similar in shape to the basidia, but slightly smaller. *Gloeocystidia* 15–30 × 5–10 µm, present at dissepiment edge, cylindrical or clavate. *Cheilocystidia*12–25 × 5–12 µm, present at dissepiment edge, irregular to broom-shaped with small diverticulate projections on the sides and at the apex, thin-walled. *Pileipellis* hyphae subparallel, smooth to diverticulate, thin-walled, 3–6 µm diam.; terminal cells cystidioid or irregular with obtuse diverticulate projections. *Tramal* hyphae subparallel along tubes, widely spaced and embedded in a thick gelatinous matrix, some with dense contents, thin-walled, 2–4 µm diam., some swollen to 8–10 µm diam. at the clavate apex. *Clamp connections* absent.

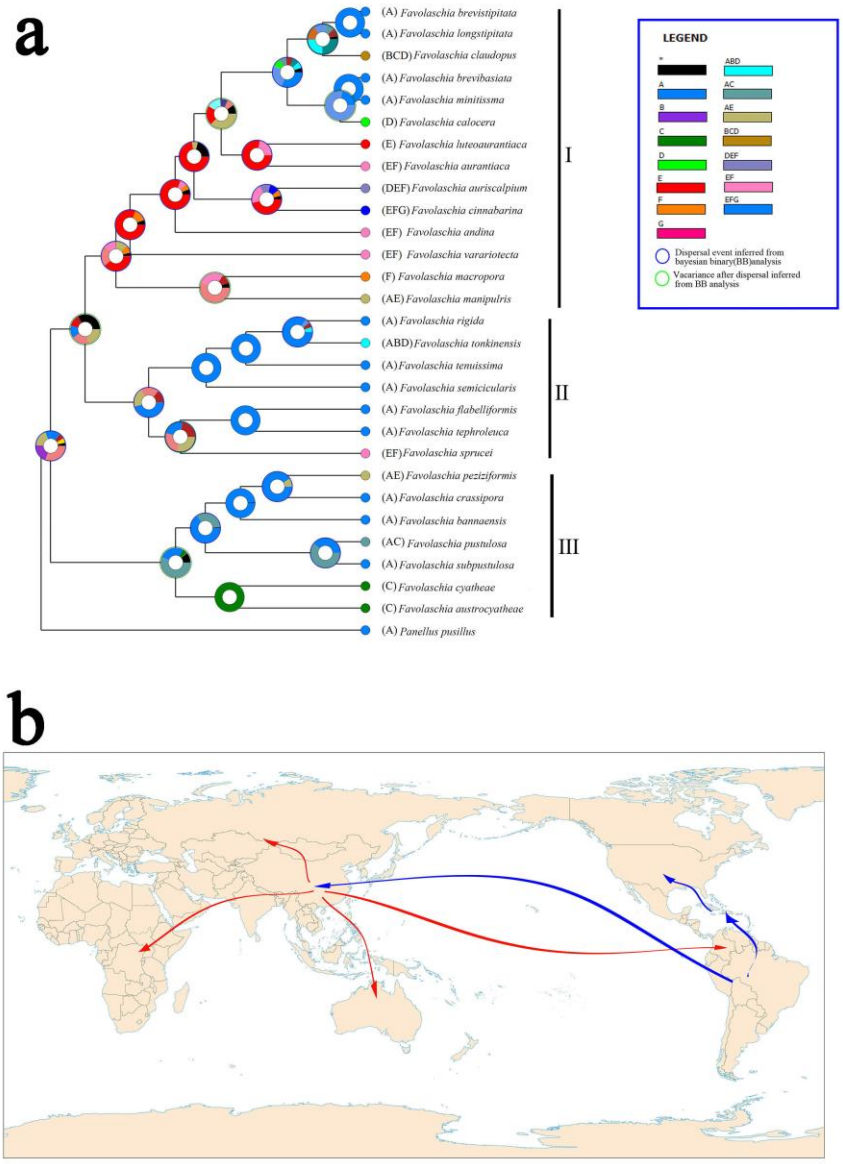

Figure 3 – a Ancestral state reconstruction and divergence time estimation of *Favolaschia* using a dataset containing ITS, nLSU and *tef1* sequences. A pie chart at each node indicates the possible

ancestral distributions inferred from dispersal-extinction-cladogenesis (DEC) analysis implemented in RASP. A black asterisk represents other ancestral ranges. b Possible dispersal routes of *Favolaschia*.

Known distribution – Subtropical regions of China.

Material examined – CHINA, Yunnan Province, Pingbian County, Daweishan National Forest Park, fallen angiosperm branch, 27 June 2019, Y. C. Dai, 26 June 2019, Dai 19769 (BJFC 031444, paratype), Dai 19871 (BJFC 031545, holotype).

Notes – *Favolaschia crassipora* was discovered in the subtropical area of Yunnan Province, China. Based on the sub-generic classification of *Favolaschia* by Singer (1974), *F. crassipora* belongs to *Favolaschia* sect. *Anechinus* subsect. *Depauperatae*, due to the absence of acanthocystidia and presence of gloeocystidia. Phylogenetically, the sequenced samples of *F. crassipora* (Dai 19871 and Dai 19769) formed an independent linage (100% ML, 1 BPP, Fig. 1), with tiny basidiocarps, small pores, thick dissepiments and big basidiospores. Morphologically, *F. sprucei* (Berk.) Singer, a species in subsect. *Depauperatae*, shares similar-sized basidiospores with *F. crassipora*, but *F. sprucei* differs in having larger basidiocarps (10–50 mm vs. 0.2–2 mm) and larger pores (0.5–2 mm vs. 0.12–0.17 mm, Singer 1974). In addition, *F. crassipora* is easily distinguished from other species in sect. *Anechinus* by the absence of clamp connections.

Favolaschia flabelliformis Q.Y. Zhang & Y.C. Dai, sp. nov. Figs 4c, 5c, 8

Index Fungorum number: IF 900428; Facesoffungi number: FoF09530

Etymology – "*flabelliformis*" (Lat.): refers to the species having a flabelliform pileus.

Basidiocarps annual, gregarious, gelatinous when fresh and dry. *Pilei* 2–3 × 1–2 mm, flabelliform or conchoid; pileal surface pale gray to grayish white (B1) when fresh, grayish (6C2–6D2) upon drying, usually fuscous near the base, plane to convex, transparent with a reticulate pattern matching the pores below, faintly pruinose when dry; margin incurved, entire; context thin, opaque, easily folded. *Hymenophore* color lighter than pileal surface, pale white (2A2) to grayish (B1) when dry, poroid, about 10–40 pores per basidiocarp; mature pores easily torn, 0.2–0.25 mm diam., round to polygonal, larger near the base and smaller near the edge, the marginal pores often incomplete; tubes up to 0.4 mm long. *Stipe* absent.

Figure 4 – Basidiocarps of *Favolaschia* species. a *F. bannaensis* (holotype). b *F. crassipora* (holotype). c *F. flabelliformis* (holotype). d *F. semicircularis* (Dai 22289) e *F. rigida* (holotype). f *F. subpustulosa* (holotype). g *F. tephroleuca* (holotype). Scale bars: a–g = 10 mm.

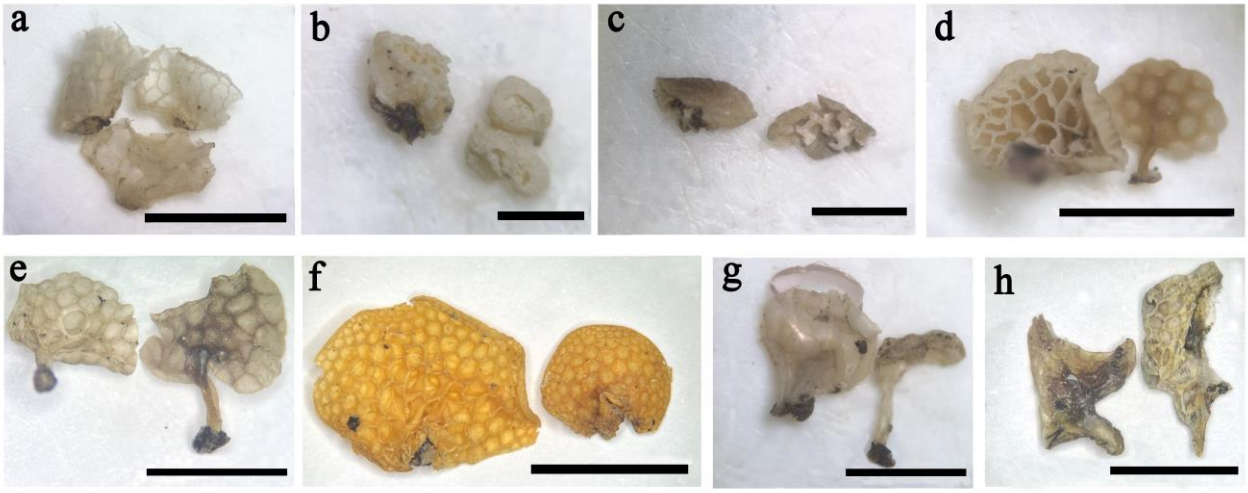

Figure 5 – Dry basidiocarps of *Favolaschia* species. a *F. bannaensis*. b *F. crassipora*. c *F. flabelliformis*. d *F. rigida*. e *F. semicircularis*. f *F. subpustulosa*. g *F. tenuissima*. h *F. tephroleuca*. Scale bars: a, d, e, g, h = 5 mm, b, c = 2 mm, f = 10 mm.

Basidiospores (7.5–)8.0–10.0(–10.2) × (5.0–)5.8–7.0(–7.8) µm, L = 8.95 µm, W = 6.30 µm, Q = 1.41–1.43 (*n* = 60/2), broadly ellipsoid, hyaline, thin-walled, smooth, with one or two guttules, faintly IKI+, CB–. *Basidia* 28.5–35 × 6.5–8 µm, cylindrical or clavate with some guttules, 2(–4)–spored, sterigmata 3–6 µm long; basidioles similar in shape to the basidia, but slightly smaller. Gloeocystidia and acanthocystidia absent. *Pileipellis* hyphae subparallel, smooth, some with dense contents, thin-walled, 4–6 µm diam. *Tramal* hyphae interwoven, widely spaced in a gelatinous matrix, some with dense contents and some collapsed, frequently branched, thin-walled, 2–4 µm diam. *Clamp connections* present.

Known distribution – Subtropical regions of China.

Material examined – CHINA, Yunnan Province, Wenshan, Maguan County, Laojunshan Nature Reserve, fallen bamboo (Bambusoideae), 30 June 2019, Y. C. Dai, Dai 20010 (BJFC031684, holotype), Dai 20016 (BJFC 031690, paratype).

Notes – *Favolaschia flabelliformis* was discovered in the subtropical area of Yunnan Province, China, and belongs to *Favolaschia* sect. *Anechinus* subsect. *Rubrinae*. Phylogenetically, two specimens of *F. flabelliformis* formed a lineage with strong support (98% ML, 1.00 BPP, Fig. 1) in our phylogeny, and are close to another new species, *F. tephroleuca*. *Favolaschia flabelliformis* resembles *F. tephroleuca* by having similar basidiospores, but the latter species has bigger basidiocarps (3–6 × 2.5–4 mm vs. 2–3 × 1–2 mm), medium gray to dark gray pileus and bigger pores (0.5–1 mm vs. 0.2–0.25 mm). Morphologically, *F. flabelliformis* and *F. aulaxina* (Mont.) Singer share a similarly colored pileus and basidiospore size. However, *F. aulaxina* differs from *F. flabelliformis* by its pores forming radially distant lamellae at edges (Singer 1974).

Favolaschia rigida Q.Y. Zhang & Y.C. Dai, sp. nov. Figs 4e, 5d, 9

Index Fungorum number: IF 900465; Facesoffungi number: FoF14234

Etymology – "*rigida*" (Lat.): refers to the species having rigid basidiocarps

Basidiocarps annual, gregarious, gelatinous when fresh, become very firm, stiff and inflexible when dry. *Pilei* 2–5 × 1–3 mm, conchoid or semicircular; pileal surface snow white (A1) when fresh, grayish (3C1) to pale yellow [4A(3–5)] upon drying, convex, transparent or semi-transparent with a reticulate pattern matching the pores below, faintly pruinose when dry; margin incurved or straight, crenulate; context thin, opaque. *Hymenophore* concolorous with pileal surface, poroid, about 45–110 pores per basidiocarp; mature pores 0.25–0.33 mm diam., hexagonal to irregular polygonal, larger near the base and smaller near the edge; tubes up to 0.4 mm long. *Stipe* grayish

(3C1) to grayish brown [6C(3–4)], usually fuscous near the base when dry, laterally attached, short, tapering to a slightly swollen base, 0–2 × 0.5–1 mm.

Basidiospores 7–9 × 5–7.8(–8) μm, L = 7.98 μm, W = 6.68 μm, Q = 1.18–1.21 (*n* = 90/3), subglobose to globose, hyaline, thin-walled, smooth, with one big guttule, faintly IKI+, CB–. *Basidia* 24–36 × 7–12 μm, clavate with some guttules, 2(–4)–spored, sterigmata 2–6 μm long; basidioles similar in shape to the basidia, but slightly smaller. Gloeocystidia and acanthocystidia absent. *Pileipellis* hyphae interwoven, smooth to diverticulate, thin-walled, 3–7 μm diam.; terminal cells cystidioid or irregularly tubular, flexuous, with constrictions or diverticulate projections on the sides and at the apex, oriented perpendicular to pileal surface. *Tramal* hyphae subparallel along tubes, widely spaced in a gelatinous matrix, occasionally with dense contents, thin-walled, 2–4 μm diam. *Hyphae in stipe* parallel along stipe, some swollen, slightly thick-walled, 4–10 μm diam. *Clamp connections* present.

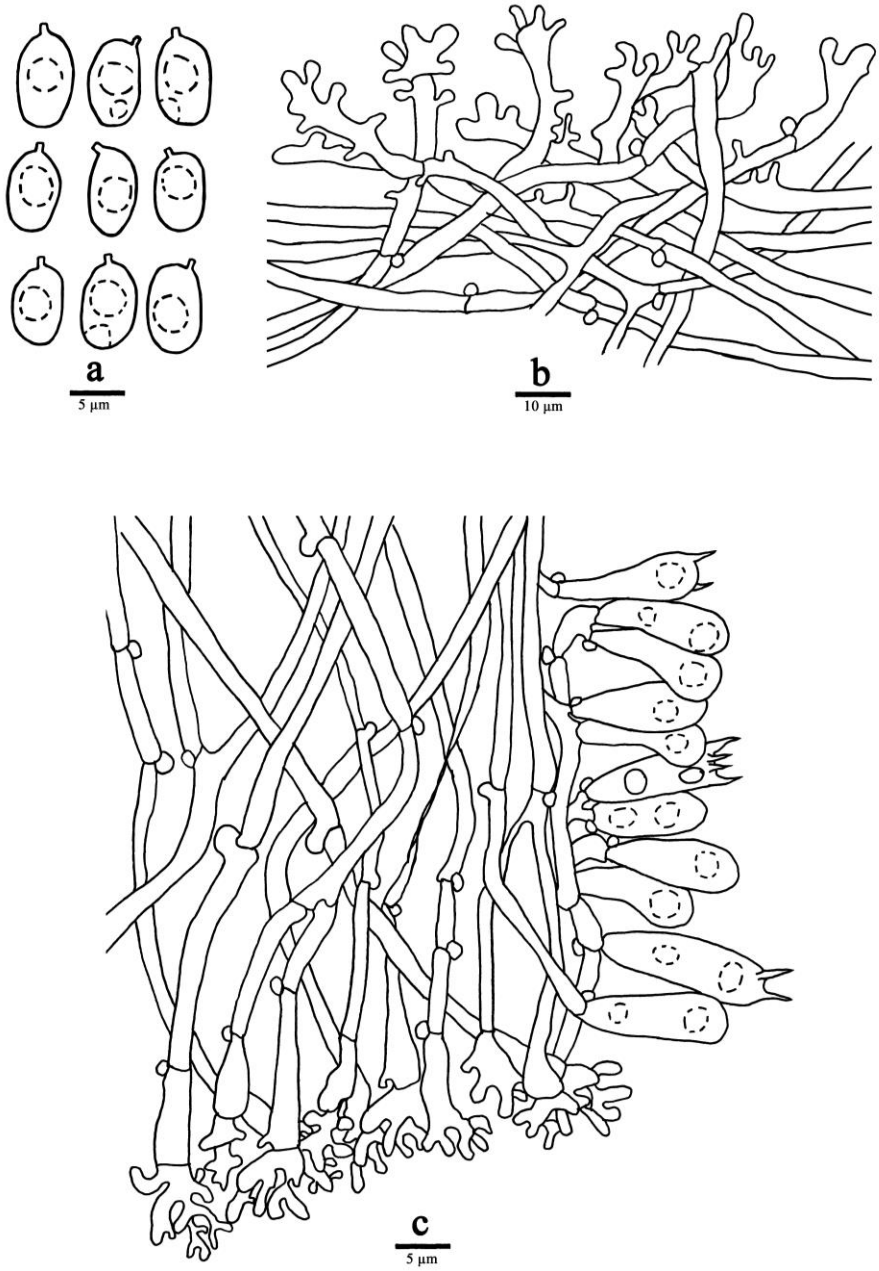

Figure 6 – Microscopic structures of *Favolaschia bannaensis* (holotype). a Basidiospores. b Hyphae and terminal cells from pileipellis. c A section of tube trama, including basidia, basidioles and cheilocystidia.

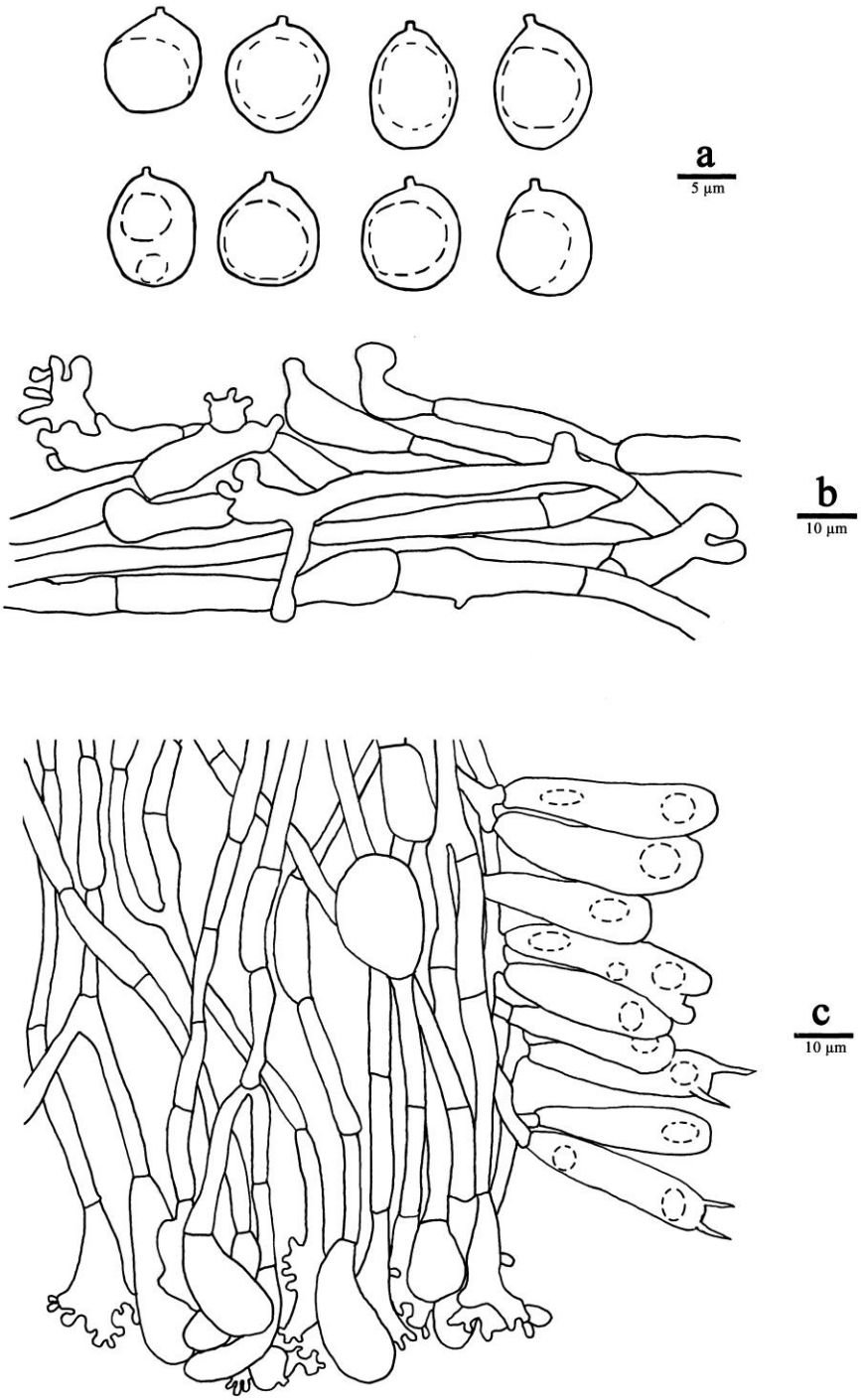

Figure 7 – Microscopic structures of *Favolaschia crassipora* (holotype). a Basidiospores. b Hyphae and terminal cells from pileipellis. c A section of tube trama, including basidia, basidioles, gloeocystidia and cheilocystidia.

Known distribution – Subtropical regions of China.

Material examined – CHINA, Fujian Province, Wuyishan, Dazhulan Scenic Spot, dead bamboo (Bambusoideae), 23 July 2021, Y. C. Dai, Dai 22614 (BJFC 037187, paratype); Guangxi, Wuzhou, Cangwu County, Tianhongfeng Forest Farm, on rotten bamboo (Bambusoideae), 29 April 2018, Dai 18566A (BJFC 027034, holotype); Yunnan Province, Jinping County, Fenshuiling Nature Reserve, dead bamboo (Bambusoideae), 18 August 2019, Y. C. Dai, Dai 20764 (BJFC 032431, paratype).

Notes – *Favolaschia rigida* was discovered in the subtropical area of China (Guangxi, Fujian, and Yunnan), and belongs to *Favolaschia* sect. *Anechinus* subsect. *Rubrinae*. Phylogenetically, samples of *F. rigida* (Dai 18566A, Dai 20764, Dai 22614) formed a highly supported linage (100% ML, 1.00 BPP, Fig. 1), that is closely related to *F. tonkinensis* and *F. tenuissima.* However, *F. tonkinensis* can be easily distinguished from *F. rigida* due to its bigger basidiocarps (6–24 mm vs. 2–5 mm), and bigger basidiospores (8–12.5 × 7–10.5 µm vs. 7–9 × 5–7.8 µm, Singer 1974). *Favolaschia rigida* and *F. tenuissima* have similar-sized basidiospores, while *F. tenuissima* differs from *F. rigida* in having abundant cheilocystidia at dissepiment edge.

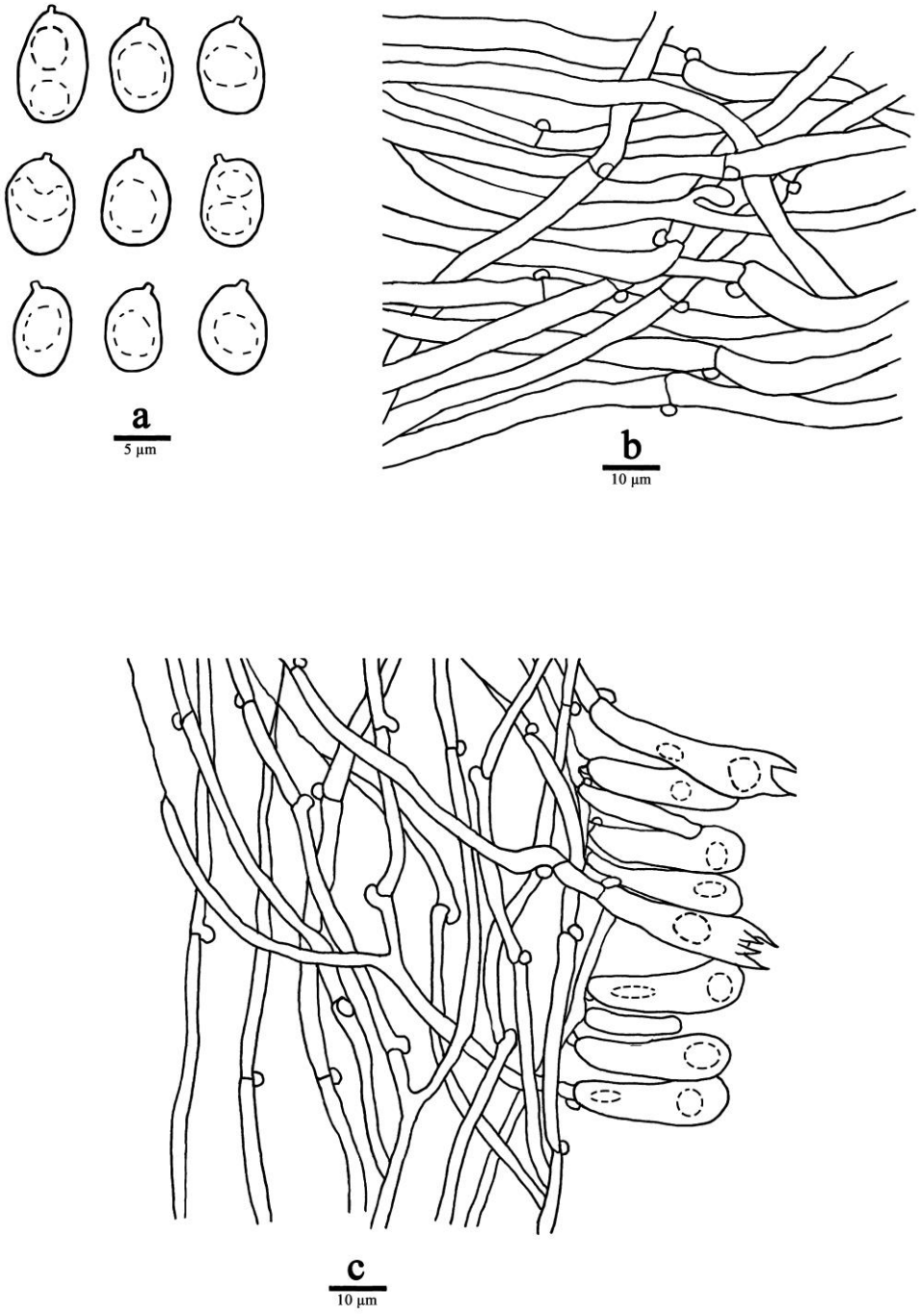

Figure 8 – Microscopic structures of *Favolaschia flabelliformis* (holotype). a Basidiospores. b Hyphae from pileipellis. c A section of tube trama, including basidia and basidioles.

Favolaschia semicircularis Q.Y. Zhang & Y.C. Dai, sp. nov. Figs 4d, 5e, 10

Index Fungorum number: IF 900466; Facesoffungi number: FoF14235

Etymology – "*semicircularis*" (Lat.): refers to the species having a semicircular pileus.

Basidiocarps annual, gregarious, gelatinous when fresh and dry. *Pilei* 3–5 × 1–3 mm, semicircular, conchoid or subcircular; pileal surface pure white to white (A1) when fresh, orange-gray (5B2–6B2) upon drying, brownish gray (5E2–5F2) near the base, depressions slightly darker than pores, convex, transparent with a reticulate pattern matching the pores below, faintly pruinose when dry; margin straight, entire or crenulate; context thin, opaque. *Hymenophore* color lighter than pileal surface, grayish yellow [1B(3–4)] when dry, poroid, about 12–75 pores per basidiocarp; mature pores 0.3–0.6 mm diam., round to polygonal, larger near the base and smaller near the edge, marginal pores often incomplete; tubes up to 0.6 mm long. *Stipe* mostly present, grayish orange [5B(3–5)], usually fuscous near the base, laterally attached, straight, subcylindrical, 1–3 × 0.5–1 mm.

Basidiospores 6–9.5(–9.8) × 4–6 μm, L = 7.66 μm, W = 5.04 μm, Q = 1.47–1.61 (*n* = 90/3), ellipsoid, hyaline, thin-walled, smooth, with one or two guttules, faintly IKI+, CB–. *Basidia* 24–32 × 5–8 μm, clavate with some guttules, 2–spored, sterigmata 5–7 μm long; basidioles similar in shape to the basidia, but slightly smaller. Gloeocystidia and acanthocystidia absent. *Cheilocystidia* 12–35 × 4–12 μm, present at dissepiment edge, clavate, fusiform or irregular with small diverticulate projections on the sides and at the apex, thin-walled. *Pileipellis* hyphae interwoven, smooth, occasionally with some small diverticulate projections at the apex, thin-walled, 5–10 μm diam. *Tramal* hyphae interwoven, widely spaced and embedded in a thick gelatinous matrix, frequently branched, some with dense contents and some collapsed, thin-walled, 2–5 μm diam. *Hyphae in stipe* subparallel along stipe, some part swollen, slightly thick-walled, 3–9 μm in diam. *Clamp connections* present.

Known distribution – Subtropical regions of China.

Material examined – CHINA, Fujian Province, Nanping, Wuyishan National Nature Reserve, dead bamboo, 19 June 2021, Y. C. Dai, Dai 22383 (BJFC 036967, paratype), rotten bamboo (Bambusoideae), Dai 22391 (BJFC 036975, paratype), Dai 22392 (BJFC 036976, paratype); Guangdong Province, Shixing County, Chebaling Nature Reserve, fallen bamboo (Bambusoideae), 14 June 2019, Y. C. Dai, Dai 19725 (BJFC 031400, paratype), Dai 19726 (BJFC 031401, paratype); Jiangxi Province, Jinggangshan, Jinggangshan Nature Reserve, Luofu Forest Farm, 5 July 2021, Y. C. Dai, Dai 22525 (BJFC 037104, paratype); Yunnan Province, Xichou County, Xiaoqiaogou Forest Farm, fallen bamboo (Bambusoideae), 29 June 2019, Y. C. Dai, Dai 19918 (BJFC 031592, paratype), Dai 19923 (BJFC 031597, holotype), Dai 19936 (BJFC 031610, paratype), Dai 19980 (BJFC 031654, paratype), Dai 19981 (BJFC 031655, paratype), fallen angiosperm branch, Dai 19939 (BJFC 031613, paratype); Zhejiang Province, Hangzhou, Fuyang District, Huanggongwang Forest Park, rotten bamboo (Bambusoideae), 2 June 2021, Y. C. Dai, Dai 22289 (BJFC036877, paratype), Dai 22290 (BJFC 036878, paratype), Dai 22291 (BJFC 036879, paratype), Dai 22298 (BJFC 036886, paratype), Dai 22302 (BJFC 036890, paratype).

Notes – 16 samples of *F. semicircularis* from subtropical China formed a highly supported linage (88% ML, 0.99 BPP, Fig. 1). The species belongs to *Favolaschia* sect. *Anechinus* subsect. *Rubrinae*. *Favolaschia peziziformis*, a species of subsect. *Rubrinae*, may be confused with *F. semicircularis* by having approximately the same basidiospore size, and strongly diverticulate hyphae in the pileipellis. However, *F. peziziformis* from Japan can be easily distinguished from *F. semicircularis* by having gloeocystidia (Kobayasi 1952, Singer 1974). *Favolaschia peziziformis* from New Zealand can be also easily distinguished from *F. semicircularis* by its larger basidiocarps (up to 10 mm vs. 3–5 mm, Singer 1974). Morphologically, *F. semicircularis* and *F. rigida* share similar basidiocarps with an opaque pileus. However, *F. rigida* can be easily distinguished from *F. semicircularis* by lacking cheilocystidia at the dissepiment edge. In addition, *F. bannaensis*, *F. semicircularis*, *F. tenuissima* and *F. tephroleuca* have similar strongly diverticulate hyphae in the pileipellis. However, *F. bannaensis* and *F. tenuissima* differ from *F. semicircularis* by their

transparent pilei. *Favolaschia tephroleuca* differs from *F. semicircularis* by its medium gray to dark gray pileus and the absence of a stipe.

Favolaschia subpustulosa Q.Y. Zhang & Y.C. Dai, sp. nov. Figs 4f, 5f, 11

Index Fungorum number: IF 900467; Facesoffungi number: FoF14236

Etymology – "*subpustulosa*" (Lat.): refers to the species being like *Favolaschia pustulosa*.

Basidiocarps annual, gregarious, gelatinous when fresh and dry. *Pilei* 10–40 × 8–30 mm, conchoid to semicircular; pileal surface snow white (1A1) when fresh, grayish orange (5B6) to golden yellow [5B(7–8)] upon drying, convex, faintly pruinose when dry; margin straight or incurved, crenulate; context thin, opaque. *Hymenophore* concolorous with pileal surface, poroid, about 80–180 pores per basidiocarp; mature pores 1–2.3 mm diam., round; tubes up to 0.6 mm long. *Stipe* absent.

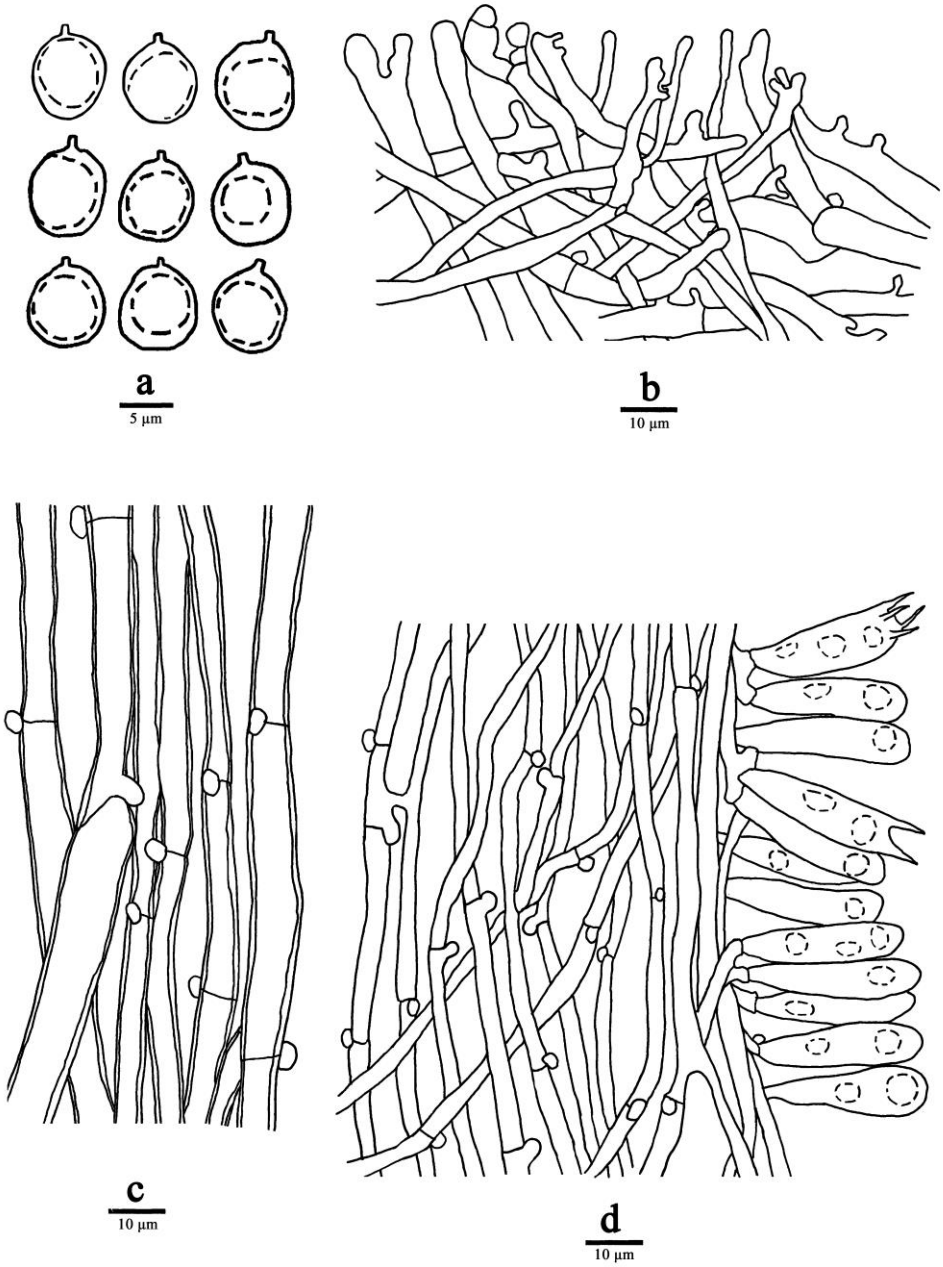

Figure 9 – Microscopic structures of *Favolaschia rigida* (holotype). a Basidiospores. b Hyphae and terminal cells from pileipellis. c Hyphae from stipe. d A section of tube trama, including basidia and basidioles.

Basidiospores (5.5–)6–7.5(–8) × 4.8–6 μm, L = 6.60 μm, W = 5.18 μm, Q = 1.27 (*n* = 30/1), broadly ellipsoid, hyaline, thin-walled, smooth, with one big guttule, faintly IKI+, CB–. *Basidia* 28–35 × 6–10 μm, cylindrical or clavate with some guttules, 2–spored, sterigmata 5–7 μm long; basidioles similar in shape to the basidia, but slightly smaller. Gloeocystidia and acanthocystidia absent. *Pileipellis* hyphae subparallel, smooth, swollen, thin-walled, 6–11 μm diam.; terminal cells cystidioid or pyriform, smooth, thin-walled. *Tramal* hyphae subparallel along tubes, widely spaced and embedded in a thick gelatinous matrix, some swollen or occasionally collapsed, thin-walled, 2–8 μm diam. *Clamp connections* present.

Known distribution – Subtropical regions of China.

Material examined – CHINA, Yunnan Province, Honghe, Lvchuan County, Huanglianshan Forest Park, angiosperm stump, 13 August 2019, Y. C. Dai, Dai 20719 (BJFC 032386, holotype).

Notes – *Favolaschia subpustulosa* was discovered in the subtropical area of Yunnan Province, China, and belongs to *Favolaschia* sect. *Anechinus* subsect. *Rubrinae*. Phylogenetically, the sample of *F. subpustulosa* (Dai 20719) formed an independent lineage and is related to *F. pustulosa* and *F.* sp. 1 (DUKE2708, DUKE2876 and DUKE3105). Morphologically, *F. pustulosa* and *F. subpustulosa* share conchoid, snow white to white basidiocarps when fresh, and similar-sized basidiospores. However, *F. pustulosa* differs from *F. subpustulosa* by its larger pores (polygonal, 3–6 mm vs. round, 1–2.3 mm).

Favolaschia tenuissima Q.Y. Zhang & Y.C. Dai, sp. nov. Figs 5g, 12

Index Fungorum number: IF 900468; Facesoffungi number: FoF14237

Etymology – "*tenuissima*" (Lat.): refers to the species having a very thin pileus.

Basidiocarps annual, gregarious, gelatinous when fresh and dry. *Pilei* 3–5 × 1–3 mm, conchoid or reniform; pileal surface white (1A1) when fresh, gray to brownish gray [6B(3–4)] upon drying, plane to convex, transparent, with a reticulate pattern matching the pores below; margin incurved, entire; context thin, transparent. *Hymenophore* concolorous with pileal surface, poroid, about 10–20 pores per basidiocarp; mature pores 0.5–1.5 mm diam., polygonal to irregular, larger near the base and smaller near the edge, the marginal pores often incomplete; tubes up to 0.3 mm long. *Stipe* obvious, concolorous with pileal surface, laterally attached, straight, subcylindrical with slightly swollen base, 1–3 × 0.5–1 mm.

Basidiospores 7–9(–9.2) × (5.8–)6–7.6(–7.8) μm, L = 8.09 μm, W = 6.65 μm, Q = 1.21–1.22 (*n* = 60/2), broadly ellipsoid to subglobose, hyaline, thin-walled, smooth, with some guttules, faintly IKI+, CB–. *Basidia* 30–40 × 8–13 μm, cylindrical or clavate with some guttules, 2–spored, sterigmata 5–12 μm long; basidioles similar in shape to the basidia, but slightly smaller. Gloeocystidia and acanthocystidia absent. *Cheilocystidia* 15–23 × 3–6 μm, present at dissepiment edge, cylindrical, tubular or irregular with small diverticulate projections on the sides and at the apex, thin-walled. *Pileipellis* hyphae interwoven, smooth to diverticulate, some with dense contents, thin-walled, 3–5 μm diam; terminal cells in shape similar to cheilocystidia, oriented perpendicular to pileal surface. *Tramal* hyphae interwoven, widely spaced in a gelatinous matrix, some with dense contents, frequently branched and collapsed, thin-walled, 2–5 μm diam. *Hyphae in stipe* subparallel along stipe, some swollen, slightly thick-walled, 2–7 μm diam. *Clamp connections* present.

Known distribution – Tropical regions of China.

Material examined – CHINA, Hainan Province, Qiongzhong County, Hainan Tropical Rainforest National Park, Limushan, dead bamboo (Bambusoideae), 11 November 2020, Y. C. Dai, Dai 22071 (BJFC 035964, holotype), Dai 22072 (BJFC 035965, paratype).

Notes – *Favolaschia tenuissima* was discovered in the tropical area of Hainan Province, China, and belongs to *Favolaschia* sect. *Anechinus* subsect. *Rubrinae*. Phylogenetically, *F. tenuissima* formed a highly supported lineage (95% ML, 1.00 BPP, Fig. 1), and then grouped with *F. rigida* and *F. tonkinensis* (Fig. 1). However, *F. rigida* can be easily distinguished from *F. tenuissima* by lacking cheilocystidia at the dissepiment edge. *F. tonkinensis* can also be easily distinguished from *F. tenuissima* due to its bigger basidiocarps (6–24 mm vs. 3–5 mm) and bigger

basidiospores (8–12.5 × 7–10.5 µm vs. 7–9 × 6–7.6 µm, Singer 1974). Morphologically, *F. bannaensis* and *F. tenuissima* share a similarly transparent pileus with strongly diverticulate hyphae in the pileipellis. However, *F. bannaensis* differs from *F. tenuissima* by its narrower basidiospores (4–6 µm vs. 6–7.6 µm in width), furthermore, they formed two distinct lineages in our phylogenies.

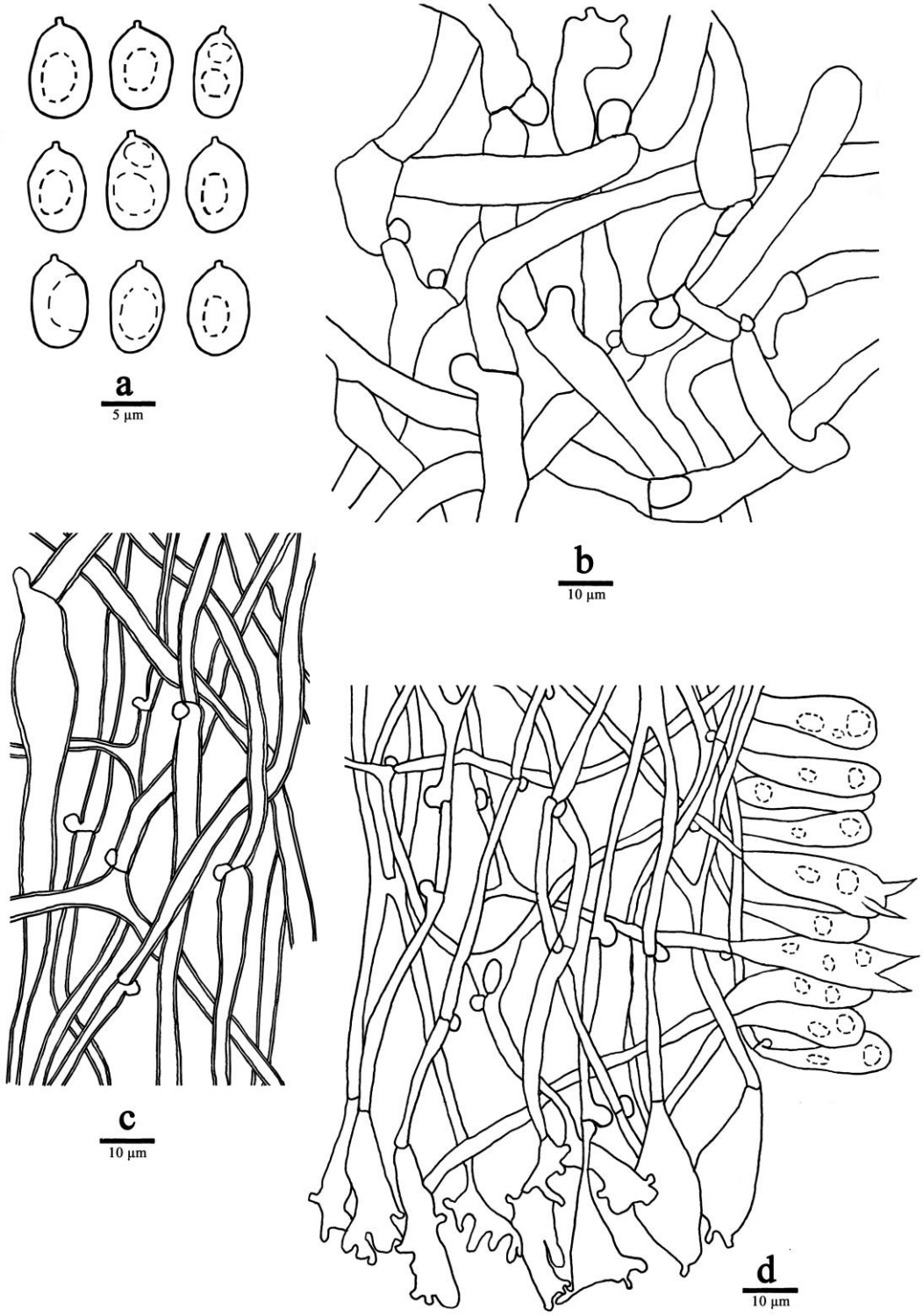

Figure 10 – Microscopic structures of *Favolaschia semicircularis* (holotype). a Basidiospores. b Hyphae from pileipellis. c Hyphae from stipe. d A section of tube trama, including basidia, basidioles and cheilocystidia.

Favolaschia tephroleuca Q.Y. Zhang & Y.C. Dai, sp. nov. Figs 4g, 5h, 13

Index Fungorum number: IF 900469; Facesoffungi number: FoF14238

Etymology – "*tephroleuca*" (Lat.): refers to the species having a medium gray to dark gray pileal surface and white pores.

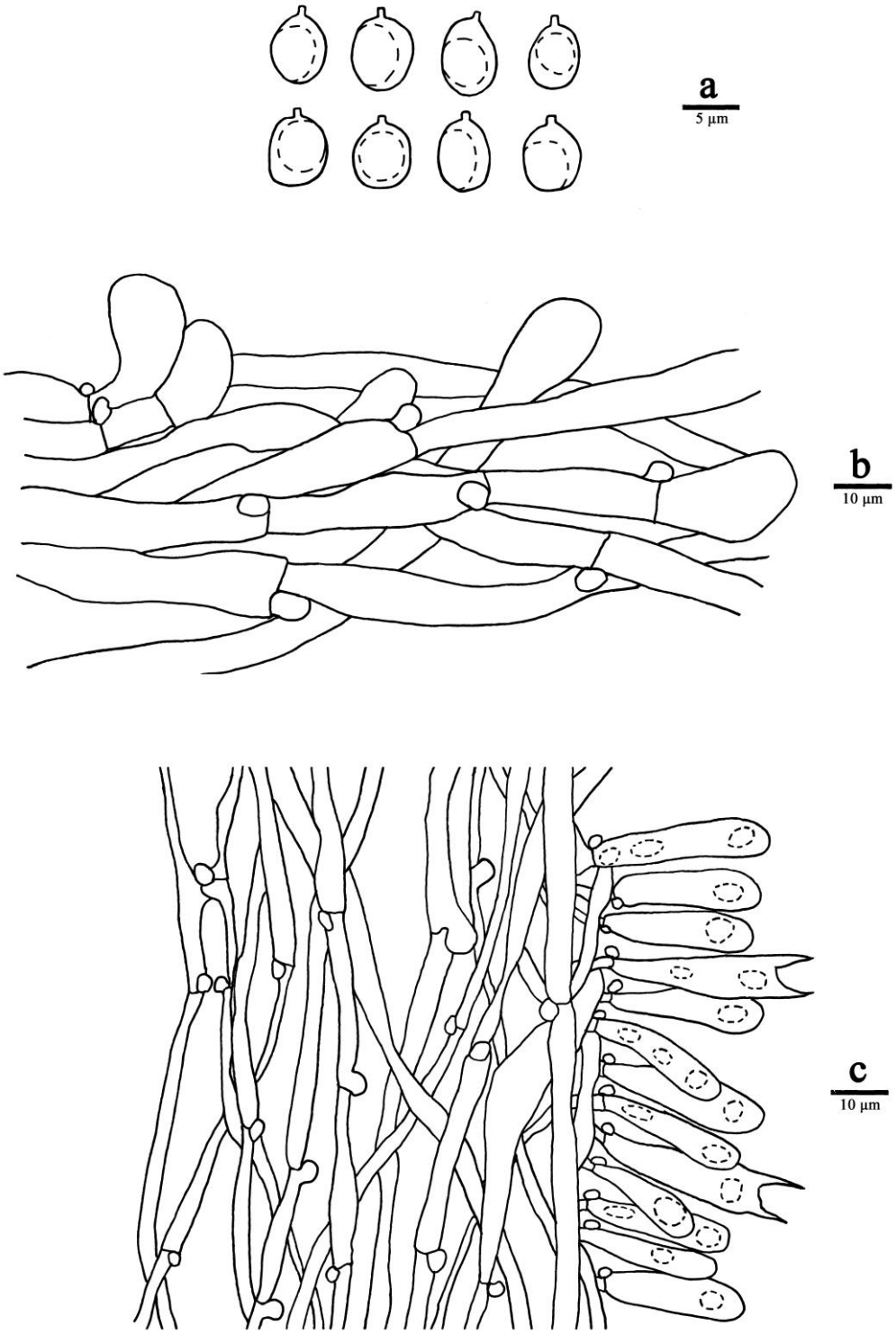

Figure 11 – Microscopic structures of *Favolaschia subpustulosa* (holotype). a Basidiospores. b Hyphae and terminal cells from pileipellis. c A section of tube trama, including basidia and basidioles.

Basidiocarps annual, gregarious, gelatinous when fresh and dry. *Pilei* 3–6 × 2.5–4 mm, conchoid or reniform; pileal surface medium gray to dark gray (1D1–1F1) when fresh, olive (1D2–1F6) to dark (1F1) when dry, pale gray (1B1–1C1) on edge, usually fuscous near the base, plane to convex, transparent with a reticulate pattern matching the pores below, faintly pruinose when dry; margin straight or incurved, crenulate; context thin, opaque. *Hymenophore* color lighter than pileal surface, whitish (1A1) to gray (5B1-5D1) when dry, poroid, about 20–40 pores per basidiocarp; mature pores 0.5–1 mm diam., round to polygonal, larger near the base and smaller near the edge, the marginal pores often incomplete; tubes up to 0.4 mm long. *Stipe* absent.

Basidiospores (7–)7.5–9.5(–9.8) × 5–7 μm, L = 8.35 μm, W = 5.97 μm, Q = 1.37 (*n* = 60/2), broadly ellipsoid, hyaline, thin-walled, smooth, with some guttules, faintly IKI+, CB–. *Basidia* 28–35 × 8–10 μm, cylindrical or clavate with some guttules, 2(–4)–spored, sterigmata 3–8 μm long; basidioles in shape similar to basidia, but slightly smaller. Gloeocystidia and acanthocystidia absent. *Cheilocystidia* 20–26 × 4–7 μm, present at dissepiment edge, tubular, broom-shaped or irregular, thin-walled, with small diverticulate projections on the sides and at the apex. *Pileipellis* hyphae interwoven, smooth to diverticulate, thin-walled, 2–5 μm diam.; terminal cells in shape similar to cheilocystidia, oriented perpendicular to pileal surface. *Tramal* hyphae subparallel along tubes, widely spaced in a gelatinous matrix, some with dense contents and some collapsed, thin-walled, 2–5 μm diam. *Clamp connections* present.

Known distribution – Temperate regions of China.

Material examined – CHINA, Chongqing, Nanzhou District, Jinfoshan, dead bamboo (Bambusoideae), 10 May 2021, Y. C. Dai, Dai 22288 (BJFC 036876, holotype); Yunnan Province, Zhaotong, Weixin County, Daxueshan Nature Reserve, fallen angiosperm twig, 16 May 2021, Y. C. Dai, Dai 22282 (BJFC 036870, paratype).

Notes – *Favolaschia tephroleuca* was discovered in temperate area of Chongqing and Yunnan, China, and belongs to *Favolaschia* sect. *Anechinus* subsect. *Rubrinae*. Morphologically, *F. torrendii* (Lloyd) Singer, a species of subsect. *Rubrinae*, shares a similar dark gray pileus color. However, *F. torrendii* can be easily distinguished *F. tephroleuca* by its smaller basidiocarps (1–2 mm vs. 3–6 mm) and smaller basidiospores (6–7.5 × 3.8–5 μm vs. 7.5–9.5 × 5–7 μm, Singer 1974).

Accuracy evaluation and variable selection in distribution prediction models

For our model, the mean value of the AUC for the training set is 0.995, which indicated favorable model performance. Table 3 shows the mean values of the relative contribution of the predictor variables in the Maxent model. Among the six parameters used for model establishment, the main environmental factors affecting the potential distribution of *Favolaschia* are precipitation of the warmest quarter (Bio18) and temperature seasonality (Bio4), with contribution rates of 68.9% and 16.7% respectively. For the above two parameters, their accumulated contribution rate reached 85.6%, indicating that those two factors played an important part in the distribution of *Favolaschia* species. The precipitation of the warmest quarter has the highest contribution rate, which indicates that rainfall is the most important factor affecting the potential distribution of *Favolaschia* species. The Jackknife result (Fig. 14) also shows that precipitation of warmest quarter (Bio18) and temperature seasonality (Bio4) are the most important predictors of *Favolaschia* species distribution in China.

Variable response curves show how each environmental variable affected the Maxent prediction, indicating how the logistic prediction changes with alteration of each environmental variable. According to the response curve (Fig. 15), a negative nonlinear response is observed for the mean diurnal range (Bio2) and a typical “S” curve is observed for the precipitation of the warmest quarter (Bio18). In addition, we obtained the optimal value of *Favolaschia* (existence probability > 0.6) for the main bioclimatic parameters, the mean diurnal range (Bio2) less than 6 °C; isothermality (Bio3) ranged from 35–45 V; the optimum value for temperature seasonality (Bio4) ranged from 3–5 °C; mean temperature of the wettest quarter (Bio8) varied from 20–25 °C; precipitation of the driest month (Bio14) ranged from above 300 mm; and precipitation of the warmest quarter (Bio18) ranged from above 750 mm.

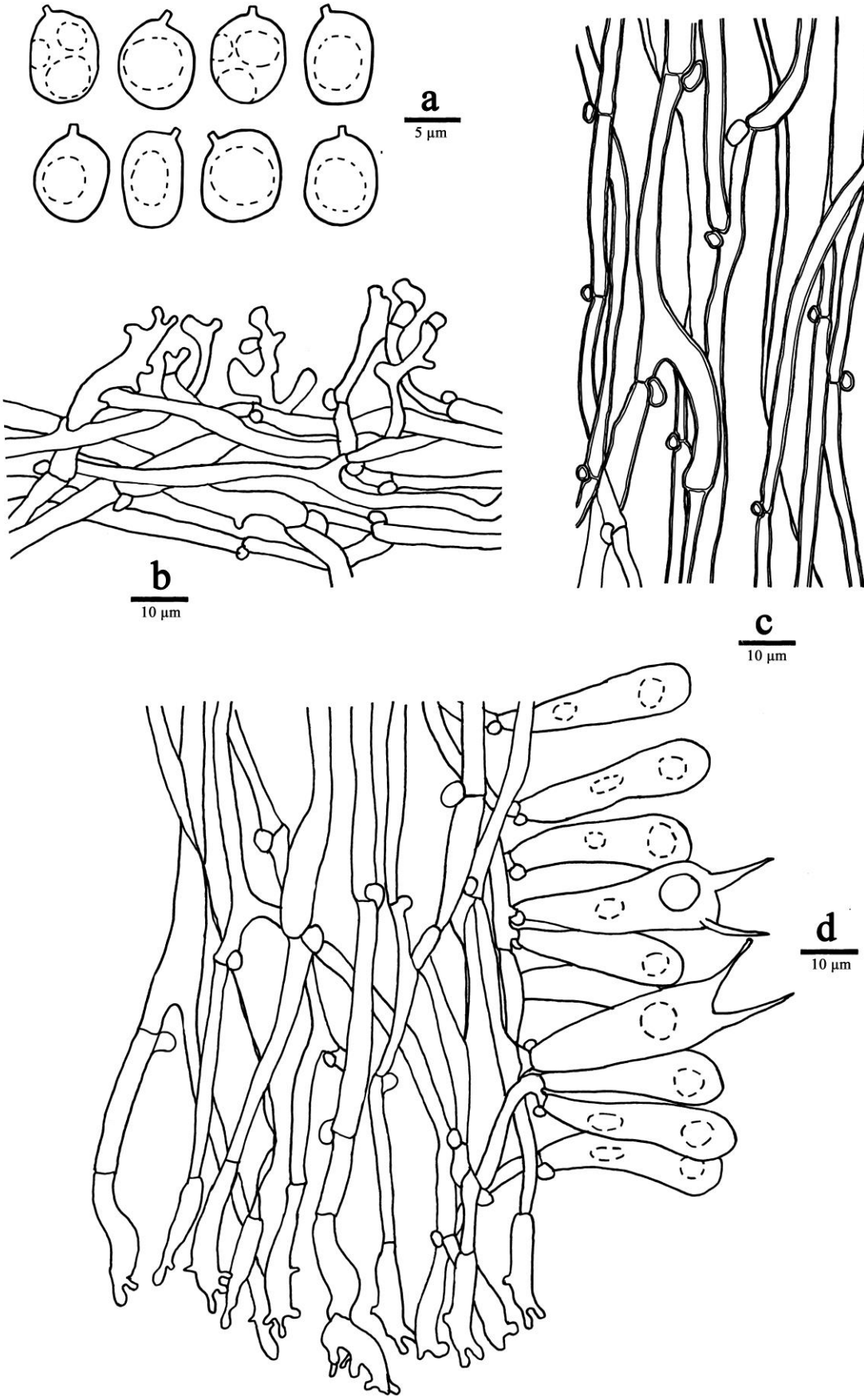

Figure 12 – Microscopic structures of *Favolaschia tenuissima* (holotype). a Basidiospores. b Hyphae and terminal cells from pileipellis. c Hyphae from stipe. d A section of tube trama, including basidia, basidioles and cheilocystidia.

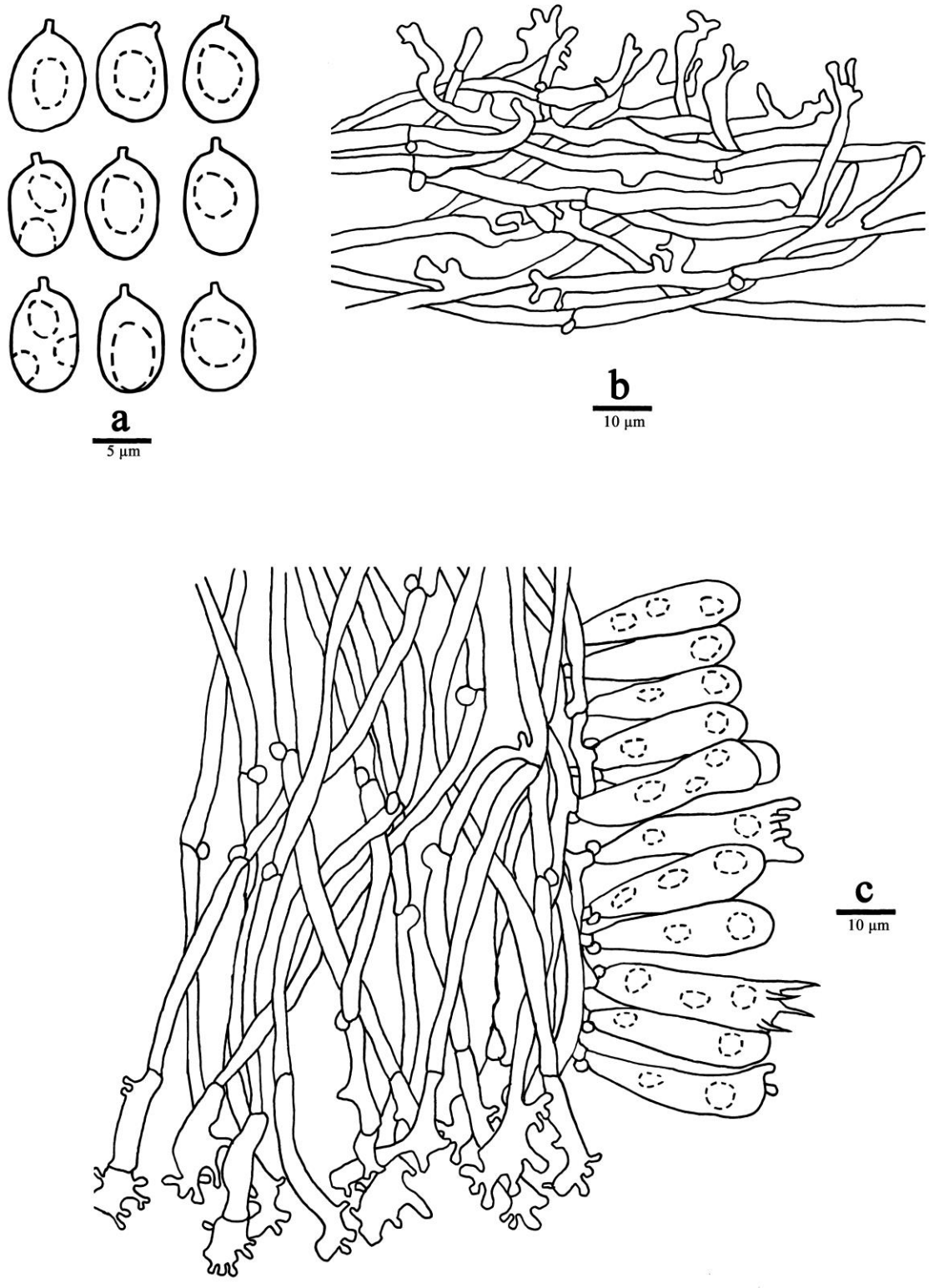

Figure 13 – Microscopic structures of *Favolaschia tephroleuca* (holotype). a Basidiospores. b Hyphae and terminal cells from pileipellis. c A section of tube trama, including basidia, basidioles and cheilocystidia.

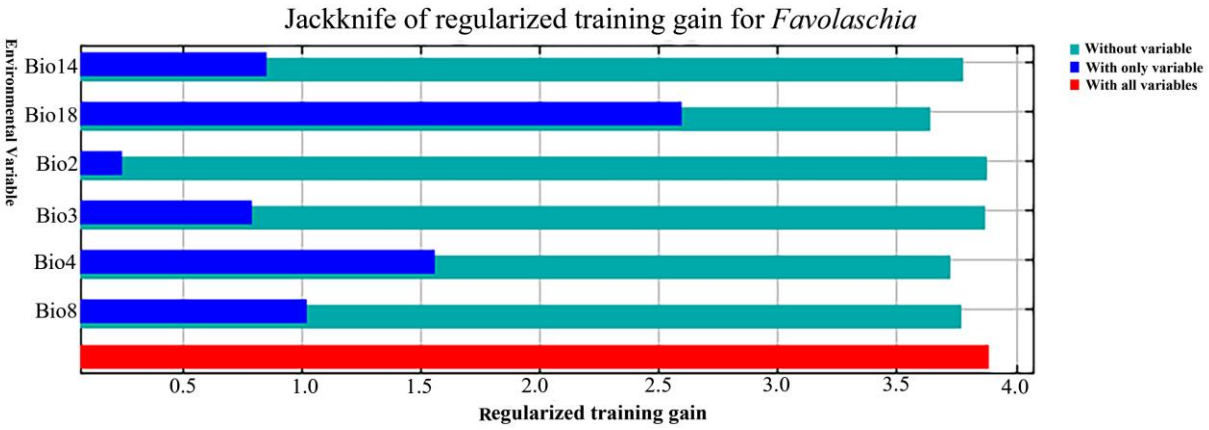

Figure 14 – The results of the Jackknife test of variables' contribution in the modelling of *Favolaschia* habitat distribution. The vertical axis represents the screened environmental variables, and the horizontal axis represents the score of each environmental variable.
Notes: The dark blue bars indicate that the gain from using each variable in isolation; the light blue bars indicate the gain lost by removing the single variable from the full model, and the red bar indicates the gain using all of the variables.

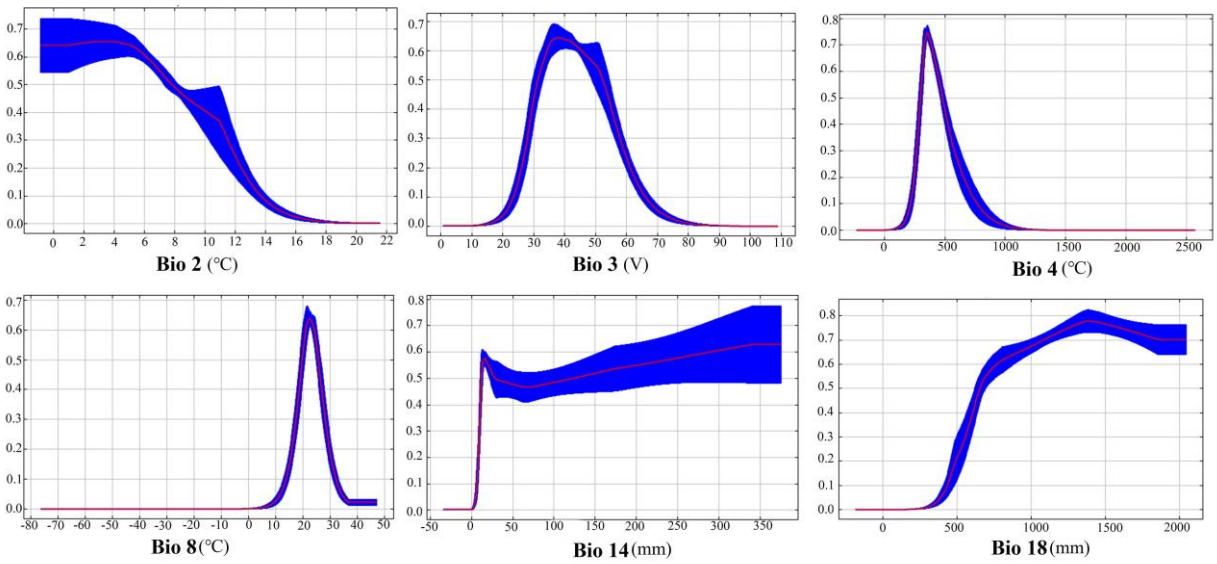

Figure 15 – Response curves of the six climate variables affecting the distribution of *Favolaschia* species in China (Bio2: mean diurnal range (mean of monthly (max temp - min temp)); Bio3: isothermality (Bio2/Bio7) (× 100); Bio4: temperature seasonality (standard deviation × 100); Bio8: mean temperature of wettest quarter; Bio14: precipitation of driest month; Bio18: precipitation of warmest quarter). Notes: Red curves show the mean response, and the blue margins indicate ±standard deviation, which was calculated over 10 replicates.

Predicted distribution of *Favolaschia* species in China

The current potential geographical distributions of *Favolaschia* species in China shown in Fig. 17, coincide with the actual distribution (Fig. 16). In general, the suitability distribution of *Favolaschia* species is located in the south of the "Qinling Mountains-Huaihe River Line" in China. The percent of area of marginal, low, medium, and high suitability distribution are 10.04%, 6.88%, 5.22%, and 1.44%, respectively (Table 4). The high suitability areas are mainly in most areas of Hainan and Taiwan Provinces, and sporadic regions of Yunnan, Guizhou, Guangxi, Guangdong,

and Tibet; the medium suitability areas are close to the high suitability areas, and extend to parts of Sichuan, Guangxi, and Fujian Provinces or Autonomous Region.; the low suitability areas are located in the middle of the medium suitability areas and marginal suitability areas, and exhibit a zonal distribution; the marginal suitability areas are mainly in the south middle of China, including Hunan, Hubei, Jiangxi, Anhui, and Jiangsu Provinces of China.

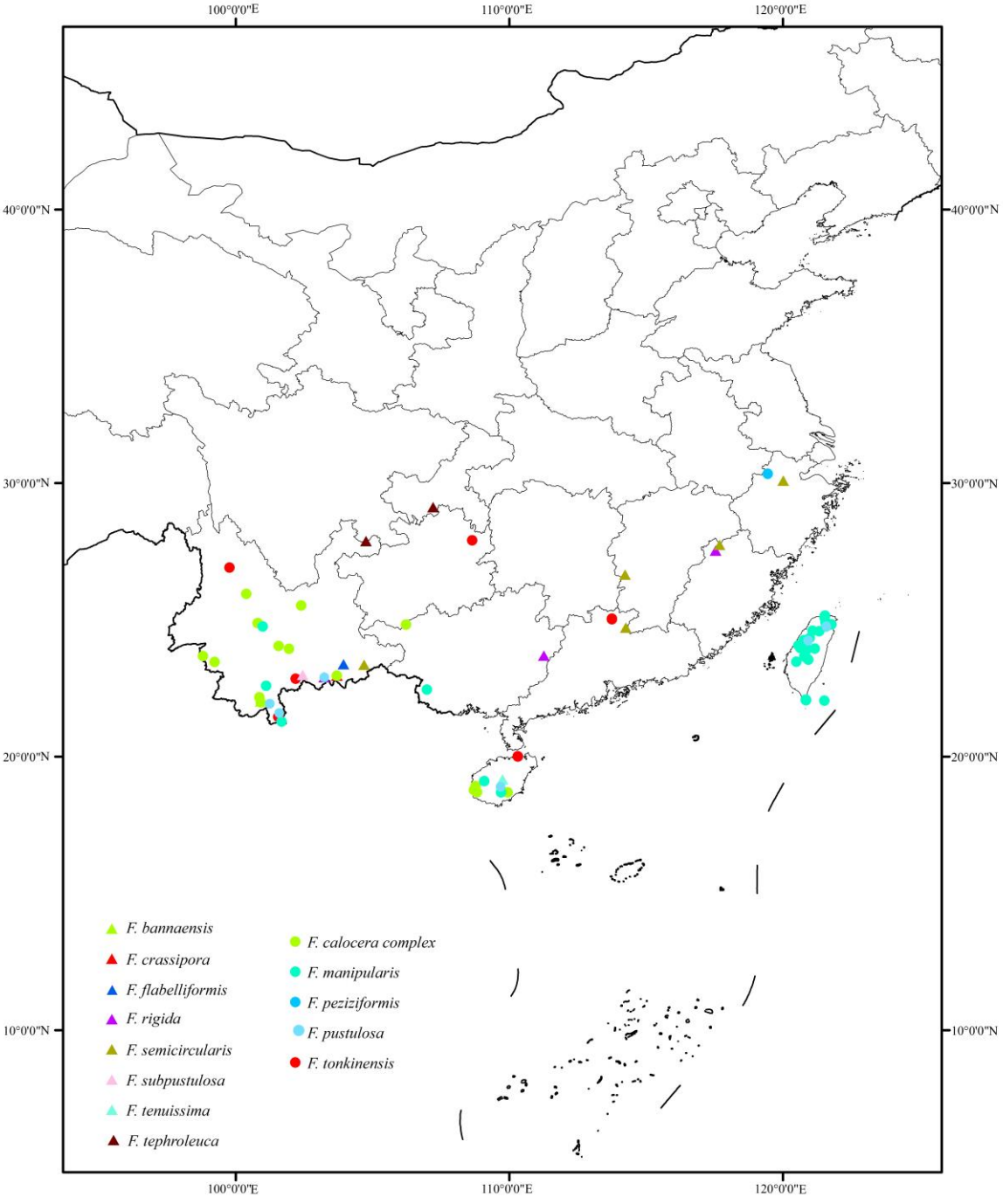

Figure 16 – Occurrence records of *Favolaschia* species in China (● represents the known Chinese *Favolaschia* species in China; ▲ represents new species in this study).

The suitability distribution area of *Favolaschia* changed markedly in the 2050s under different climate change scenarios (Fig. 18). According to the SSP126 climate change scenario, there is hardly any notable change by the 2050s, but there tends to be a decrease in the medium suitability area and an increase in the high suitability area of *Favolaschia*, which may represent a

transitional period. Compared to the current prediction, the potential distribution areas of non-suitability and marginal suitability areas gradually decreased, and the low, medium, and high suitability areas distinctly increased under the SSP245 scenario in the 2050s, which indicates that more and more areas are being transformed into areas of higher suitability. Conversely, under the SSP370 and SSP585 scenario in 2050s, the potential distribution area of marginal and low suitability increased, and the medium, and high suitability areas gradually decreased, which indicates the inhabitable environment of *Favolaschia* will shrink in the future under the higher greenhouse gas emissions.

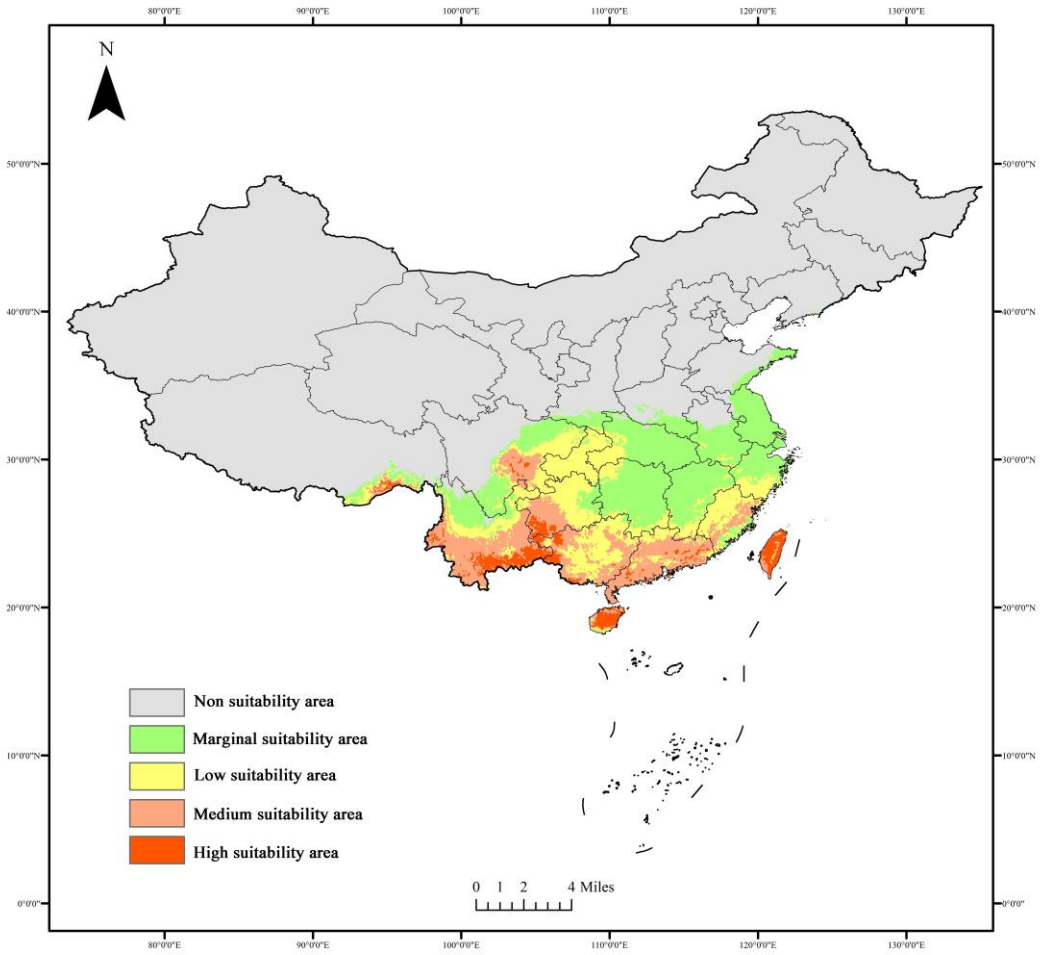

Figure 17 – Prediction of potential suitability distribution areas for *Favolaschia* species during the current time in China. [Non-suitability area (< 0.02), marginal suitability area (0.02–0.2), low suitability area (0.2–0.4), medium suitability area (0.4–0.6), and high suitability area (> 0.6)].

Table 4 Percentage of the predicted suitability area for the presence of *Favolaschia* species for present and the 2050s under different climate scenarios in China.

Suitability Grade	Current (%)	SSP126 2050s (%)	SSP245 2050s (%)	SSP370 2050s (%)	SSP585 2050s (%)
Non-suitability area (< 0.02)	76.40	76.49	75.96	76.67	75.97
Marginal suitability area (0.02–0.2)	10.04	11.14	7.11	11.43	10.96
Low suitability area (0.2–0.4)	6.89	6.69	7.40	7.28	8.11
Medium suitability area (0.4–0.6)	5.22	3.99	7.11	3.60	4.08
High suitability area (> 0.6)	1.44	1.67	2.42	1.01	0.88

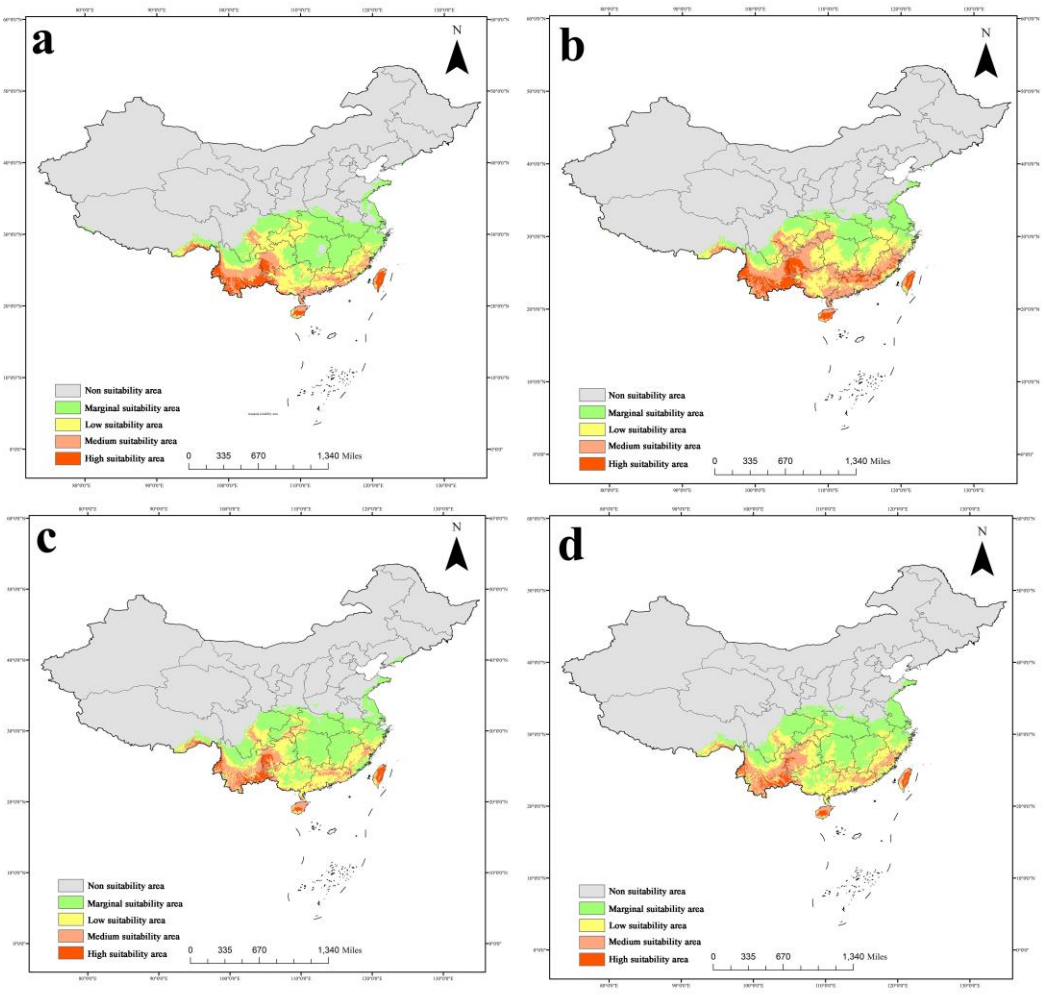

Figure 18 – Prediction of potential suitability distribution areas for *Favolaschia* during the 2050s under different climate scenarios in China. (SSP: Shared Socio-economic Pathways, a SSP126 scenario. b SSP245 scenario. c SSP370 scenario. d SSP585 scenario).

Discussion

In this study, we investigated the phylogeny, biogeographic patterns, as well as potential geographic distribution of the genus *Favolaschia*. Our data updates the taxonomy and phylogeny of *Favolaschia* in China and proposes eight new species based on both morphology and molecular phylogenetic analysis. An identification key is provided for all the 16 *Favolaschia* species found in China. We compared the Chinese (East Asia) samples with those previously identified species from Oceania, South and Central America, and Africa. The analyses of such a comprehensive collection from the wide geographic range of *Favolaschia* in China allowed an unprecedented inference of the species diversity, phylogeny, distribution pattern and the evolutionary history of this important fungal group.

Taxonomic diversity and phylogenetic analyses of *Favolaschia*

The distribution of these Chinese *Favolaschia* species is shows in Fig. 16. *Favolaschia brevibasidiata*, *F. brevistipitata*, *F. longistipitata*, and *F. minutissima* belong to the *Favolaschia calocera* complex, and they are conspicuous because of their orange and yellow basidiocarps; *F. pustulosa* and *F. manipularis* are obvious by their pure white and large basidiocarps, and growth on stumps of angiosperm trees; *F. tonkinensis* is prevalent in tropical China, with various basidiocarp morphology (shape from conchoid, subcircular to irregular; color from white, medium gray to dark gray; stipe present or absent), and grows gregariously on dead bamboo; *F. peziziformis* is common on leaves or dead stems of Palmae.

Singer (1974) divided *Favolaschia* into two sections (sect. *Favolaschia* and sect. *Anechinus*) and in our phylogeny, taxa in the monophyletic group A and polyphyletic group B (Fig. 1) correspond to these two sections. Morphologically, species in group A, including the *F. calocera* complex, are distinguished by brightly pigmented basidiocarps, conspicuous gloeocystidia, and distinct acanthocystidia. Species in group B, including the eight new species in this study, are characterized by lacking acanthocystidia or having them replaced by diverticulate hyphae. The sect. *Anechinus* includes two morphologically separated subsections, subsect. *Rubrinae* and subsect. *Depauperatae*; the gloeocystidia or gloeoplerous hyphae are absent in the former but present in the latter. However, these two subsections do not form monophyletic clades in our phylogeny (Fig. 1, group B1 and B2).

The species composition of *Favolaschia* in China is distinctly different from that in South America. Singer's 51 accepted species and several subspecies or varieties in the genus, mainly rests on an intensive study in 1974 of the neotropical collections with only four neotropical species accepted in *Favolaschia* sect. *Anechinus* (Singer 1974). Gillen et al. (2012) and Magnago et al. (2013) summarized *Favolaschia* species from Brazil, Ecuador, and Panama, and no species match sect. *Anechinus*. Conversely, most Chinese *Favolaschia* species match sect. *Anechinus* except the *Favolaschia calocera* complex. It is still noteworthy that *F. calocera* has always been considered to be an invasive fungus by several countries (Heim 1945; Johnston et al. 1998, 2006; Chuzho & Dkhar 2018). Outside its type locality in Madagascar, it has spread to Europe in the past couple of decades (Vizzini & Zotti 2002; Vizzini et al. 2009). It is also common in tropical China and displays a higher genetic variability (Zhang & Dai 2021). Therefore, our investigations on the Chinese *Favolaschia* species show that the diversity of *Favolaschia* in China was underestimated previously. Accordingly, we presume that more new species of *Favolaschia* sect. *Anechinus* exist in China, and intensive investigations on taxonomy and phylogeny are still needed to identify all the *Favolaschia* species.

Key to 16 species of *Favolaschia* found in China

1. Acanthocystidia present 2
1. Acanthocystidia absent 5
2. Basidiocarps apricot orange when fresh 3
2. Basidiocarps lemon chrome when fresh 4
3. Pileus usually <5 mm ..... *F. minutissima*
3. Pileus usually >5 mm ..... *F. brevibasidiata*
4. Stipe usually <5 mm long ..... *F. brevistipitata*
4. Stipe usually >5 mm long ..... *F. longistipitata*
5. Basidiocarps campanulate ..... *F. manipularis*
5. Basidiocarps conchoid, flabellate, reniform, semicircular or subcircular 6
6. Mature pileus > 2 cm 7
6. Mature pileus < 2 cm 9
7. Stipe present ..... *F. tonkinensis*
7. Stipe absent 8
8. Mature pores polygonal, 3–6 mm in width ..... *F. pustulosa*
8. Mature pores round, 1–2.3 mm in width ..... *F. subpustulosa*
9. Gloeocystidia present 10
9. Gloeocystidia absent 11
10. Basidiospores 4.5–5.5 μm in width ..... *F. peziziformis*
10. Basidiospores 7–10 μm in width ..... *F. crassipora*
11. Pileus transparent 12
11. Pileus opaque 13
12. Stipe obvious, 1–3 × 0.5–1 mm ..... *F. tenuissima*
12. Stipe absent ..... *F. bannaensis*

13. Pileus ash gray to fuscous or dark when fresh.....*F. tephroleuca*
13. Pileus usually white to pale white when fresh..... 14
14. Cheilocystidia present at dissepiment edge .....*F. semicircularis*
14. Cheilocystidia absent..... 15
15. Stipe usually present, and with diverticulate hyphae in pileipellis.....*F. rigida*
15. Stipe absent, and without diverticulate hyphae in pileipellis .....*F. flabelliformis*

Possible origin of *Favolaschia*

Our analysis of divergence times using a dataset of two ribosomal RNA genes (ITS and nLSU rDNA) and one protein-coding gene (*tef1*) suggests that *Favolaschia* possibly emerged in the Paleogene with a mean stem age of 49.6 Mya (95% HPD of 36.7–75.7 Mya), and East Asia and South and Central America are inferred to be the most probable ancestral areas (Fig. 3). Indeed, the divergence of major groups within *Favolaschia* occurred mainly during the Miocene to Oligocene. Stochastic changes in temperature and aridification in the Miocene might have led to the population expansions and contractions of many organisms in small regions (refugia) (Yang 2005, Chen et al. 2015).

South America is the center of origin for group I (23.3 Mya, 95% HPD of 17.5–30.1 Mya) and contains some old relicts that contributed to its high endemism of *Favolaschia* in the region. Six species, *F. brevibasidiata*, *F. brevistipitata*, *F. longistipitata*, *F. calocera*, *F. claudopus* (Singer) Q.Y. Zhang & C. Dai, and *F. minutissima* belong to the *F. calocera* complex and are closely related (Fig. 3a), indicating the dispersal route of South America–East Asia–Africa. The natural distribution of the *F. calocera* complex is a controversial question, which has been explored by many taxonomists (Johnston et al. 2006, Vizzini et al. 2009). Moreover, due to the fact that the *F. calocera* complex is particularly common in modified and anthropically disturbed sites such as forest remnants, it also seems to have experienced some human-mediated dispersal in Oceania (Vizzini et al. 2009). Johnston et al. (1998, 2006) mentioned that the *F. calocera* complex spread to Australia and New Zealand presumably by shipped timber. In addition, species in group I with another Pan-American distribution exhibit a South America–Central America–North America dispersal route. Our results suggest that multiple dispersals via the Bering Land Bridge and regional speciation after vicariance due to changing climate conditions during the middle Miocene through early Pliocene likely contributed significantly to the occurrences and endemism of some *Favolaschia* species in Central and North America. The third intercontinental distribution between South America and East Asia is exhibited in species *F. manipularis*, with an estimated divergence time of 15.8 Mya.

East Asia is the center of origin for group II (22.4 Mya, 95% HPD of 15.9–29.7 Mya). This group contains five new species, viz., *Favolaschia rigida*, *F. tenuissima*, *F. semicircularis*, *F. flabelliformis*, and *F. tephroleuca*, from China, and one species, *F. sprucei* (Berk.) Singer, from South America (Fig. 3a). It is notable that *F. sprucei* does not form a robust sister relationship with other species in our phylogeny (Fig. 1). Although the estimated divergence time is potentially inaccurate, the dispersal route between East Asia and South and Central America is proposed. Moreover, *F. tonkinensis* exhibits a continuous distribution in Africa, Oceania and East Asia (Fig. 3a). The DEC analysis inferred East Asia to be the origin for this clade, with an estimated divergence time of 7.6 Mya.

In group III, East Asia and Oceania are estimated to the center of origin (23.7 Mya, 95% HPD of 15.8–33.3 Mya). Two species, *F. austrocyatheae* P.R. Johnst. and *F. cyatheae* P.R. Johnst., found in subtropical New Zealand (Oceania), form a basal linage. These two species show significant divergence from other taxa in this group, which infers an East Asia–Oceania dispersal route. We deduced that the increase in tropical forests area associated with the Miocene warming trend may be an important factor for species exchanges between Asia and Oceania. In addition, *F. peziziformis* also exhibits a continuous distribution in East Asia and South America (Fig. 3), with an estimated divergence time of 9.6 Mya.

Key environmental factors and predicted distribution of *Favolaschia*

In terms of biodiversity and ecology of the genus *Favolaschia*, it is important to determine which environmental factors shape and maintain the geographical distribution. As suggested by our results (Table 3), precipitation-variable (precipitation in the warmest quarter, Bio18) has a most important impact on the potential distribution of *Favolaschia* species, which provide 71% contribution to model performance. It indicates that *Favolaschia* species are all sensitive to moisture in the growing season. As demonstrated in our investigation in China, every region where a *Favolaschia* species might exist was shown to have a rainy season with consistently high humidity during the growing season, which possibly provides a suitable environment for growth of this gelatinous genus. Besides precipitation, temperature is the other clearly major determinant of both plant and animal distributions (Crick & Sparks 1999, Easterling et al. 2000, Walther et al. 2002). The variable with the second highest predictive power in the Maxent analyses for the *Favolaschia* species is temperature seasonality (Bio4), which provides 19.4% contribution to model performance. For distribution of *Favolaschia* species mainly in tropical to subtropical areas, temperature-seasonality plays an important role in its distribution.

Based on the Maxent model, *Favolaschia* species are mostly distributed across subtropical regions in the southern "Qinling Mountains-Huaihe River Line" (Fig. 17). Generally, "the Qinling Mountains-Huaihe River Line" serves as the boundary of the subtropical and warm temperate zones, the temperate subtropical monsoon climates, and the 0 °C isotherm in January across China (Yang 2013, Kong et al. 2021). In general situations, the north part of this area is different from the south in terms of precipitation, temperature, river discharge, humidity, vegetation type, soil type, and topography. Notably, the climate south of this line features ample heat and moisture, a humid climate, and heat and rain at the same time, which are the leading climatic parameters that restrict the distribution of *Favolaschia* species. As suggested by the model result, the predicted potential suitability distribution area of *Favolaschia* species of the present time matched the actual occurrence well, the high suitability regions were mainly located at coastal areas of southwestern China, as well as the Hainan and Taiwan Province of China. On the basis of the present suitability distribution of *Favolaschia*, it will markedly change in the 2050s period under different climate change scenarios. Our results indicate that temperature has a positive effect on *Favolaschia* species, but, a continuous rise in temperature might have a negative effect.

However, our study has several limitations that deserve to be mentioned. Maxent model generally interprets the basic nature of the niches of species, rather than the actual niches (Yang et al. 2013, Yuan et al. 2015). A number of factors that affect the dimension of an actual niche are not taken into consideration in the prediction of potential geographical distributions of many species. In this study, certain parameters affecting the distribution of *Favolaschia* species are not considered, such as the effect of competition between species, geographical obstruction, and anthropogenic impact (Pearson 2007, Sunil & Thomas 2009). As a result, research in the future should take such parameters into consideration. Then, some studies have shown that sample sizes can affect the performance of species distribution models, and the results will probably be unsatisfactory if few records are used (Pearce & Ferrier 2000, Kadmon et al. 2003, Hernandez et al. 2006). However, Maxent reportedly provides acceptable power for predicting distributions even with very few records, for instance < 10, at least in some cases (Wisz et al. 2008, Shcheglovitova & Anderson 2013). Furthermore, most of the previous research has focused on distribution prediction to species level. However, *Favolaschia* species have similar evolutionary trends, relatively stable taxonomic characteristics and distribution, and are relatively difficult to collect due to a short growth period. Therefore, we investigated the potential suitable areas of *Favolaschia* at genus level in China.

Overall, conclusions here of potential geographical distributions of the genus are only preliminary, which could provide valuable help in searching for the *Favolaschia* in areas where it is hitherto unknown, and the biological diversity. With further research and more *Favolaschia* species distribution sites in China, we can obtain more accurate and reliable prediction results.

Acknowledgements

The research was supported by the National Natural Science Foundation of China (Project Nos. 32161143013 and U1802231).

References

Adhikari D, Barik SK, Upadhaya K. 2012 – Habitat distribution modelling for reintroduction of Ilex khasiana Purk., a critically endangered tree species of northeastern India. Ecological Engineering 40, 37–43. Doi 10.1016/j.ecoleng.2011.12.004

Berbee ML, Taylor JW. 2010 – Dating the molecular clock in fungi – how close are we? Fungal Biology Reviews 24, 1–16. Doi 10.1016/j.fbr.2010.03.001

Bouckaert R, Heled J, Kühnert D, Vaughan T et al. 2014 – BEAST 2: a software platform for Bayesian evolutionary analysis. PLoS Computational Biology 10, e1003537. Doi 10.1371/journal.pcbi.1003537

Cai Q, Tulloss RE, Tang LP, Tolgor B et al. 2014 – Multi-locus phylogeny of lethal amanitas: implications for species diversity and historical biogeography. BMC Evolutionary Biology 14, 1–16. Doi 10.1186/1471-2148-14-143

Chen JJ, Cui BK, Zhou LW, Korhonen K, Dai YC. 2015 – Phylogeny, divergence time estimation, and biogeography of the genus *Heterobasidion* (Basidiomycota, Russulales). Fungal Diversity 71, 185–200.

Chew ALC, Tan YS, Desjardin DE, Musa MY, Sabaratnam V. 2014 – Four new bioluminescent taxa of *Mycena* sect. *Calodontes* from Peninsular Malaysia. Mycologia 106, 976–988. Doi 10.3852/13-274

Chuzho K, Dkhar MS. 2018 – Ecological determinants of wood-rotting fungal diversity and first report of *Favolaschia calocera*, an invasive species from India. Proceedings of the National Academy of Sciences 89, 1177–1188. Doi 10.1007/s40011-018-1038-1

Clémençon H. 1977 – Anatomie der Hymenomyceten (Anatomy of the Hymenomycetes); Flück-Wirth Teufen, Ed.; Universität Lausanne: Lausanne, Switzerland.

Crick HQP, Sparks TH. 1999 – Climate change related to egg-laying trends. Nature 399, 423–424. Doi 10.1038/20839

Easterling DR, Meehl GA, Parmesan C, Changnon SA et al. 2000 – Climate extremes: observations, modeling, and impacts. Science 289, 2068–2074. Doi 10.1126/science.289.5487.2068

Elith J, Graham HC, Anderson PR, Dudik M et al. 2006 – Novel methods improve prediction of species' distributions from occurrence data. Ecography 29, 129–151. Doi 10.1111/j.2006.0906-7590.04596.x

Floudas D, Binder M, Riley R, Barry K et al. 2012 – The Paleozonic origin of enzymatic lignin decomposition reconstructed from 31 fungal genomes. Science 336, 1715–1719. Doi 10.1126/science.1221748

Ganeshaiah KN, Barve N, Nath N, Chandrashekara K et al. 2003 – Predicting the potential geographical distribution of the sugarcane woolly aphid Using GARP and DIVA-GIS. Current Science 85, 1526–1528.

Gillen K, Laessoe T, Kirschner R, Piepenbring M. 2012 – *Favolaschia* species (Agaricales, Basidiomycota) from Ecuador and Panama. Nova Hedwig 96, 117–165. Doi 10.1127/0029-5035/2012/0070

Graham CH, Moritz C, Williams SE. 2006 – Habitat history improves prediction of biodiversity in a rainforest fauna. Proceedings of the National Academy of Sciences 103, 632–636. Doi 10.1073/pnas.0505754103

Hall TA. 1999 – BioEdit: a user-friendly biological sequence alignment editor and analysis program for Windows 95/98/NT. Nucleic Acids Symposium Series 41, 95–98.

Heim R. 1945 – Les Agarics tropicaux a hyménium tubule (Madagascar, Côte d'lvoire, Guinée, Antilles, Insulinde). Revue de Mycologie 10, 3–61.

Hernandez PA, Graham CH, Master LL, Albert DL. 2006 – The effect of sample size and species characteristics on performance of different species distribution modeling methods. Ecography 29, 773–785. Doi 10.1111/j.0906-7590.2006.04700.x
Hibbett DS, Grimaldi D, Donoghue MJ. 1995 – Cretaceous mushrooms in amber. Nature 377, 487–487. Doi 10.1038/377487a0
Hibbett DS, Grimaldi D, Donoghue MJ. 1997 – Fossil mushrooms from Miocene and Cretaceous ambers and the evolution of Homobasidiomycetes. American Journal of Botany 84, 981–991. Doi 10.2307/2446289
Hillis DM, Bull JJ. 1993 – An empirical test of bootstrapping as a method for assessing confidence in phylogenetic analysis. Systematic biology 42: 182–192. Doi 10.1093/sysbio/42.2.182
Hosaka K, Castellano MA, Spatafora JW. 2008 – Biogeography of Hysterangiales (Phallomycetidae, Basidiomycota). Mycological Research 112, 448–462. Doi 10.1016/j.mycres.2007.06.004
Jiang T, Lu R, Huang JL, Wang Y et al. 2020 – New scenarios of CMIP6 model (SSP-RCP) and its application in the Huaihe river basin. Advances in Meteorological Science and Technology 10, 102−109.
Johnston PR, Whitton SR, Buchanan PK, Park D, Moncalvo JM. 2006 – The basidiomycete genus *Favolaschia* in New Zealand. New Zealand Journal of Botany 44, 65–87. Doi 10.1080/0028825X.2006.9513007
Johnston PR, Buchanan PK, Leathwick J, Mortimer S. 1998 – Fungal invaders. Australasian Mycological Newsletter 17, 48–52.
Kadmon R, Farber O, Danin A. 2003 – A systematic analysis of factors affecting the performance of climatic envelope models. Ecological Applications 13, 853–867. Doi 10.1890/1051-0761(2003)013
Kirk PM, Cannon PF, Minter DW, Stalpers JA. 2008 – Dictionary of the fungi, 10th ed. CAB International, Wallingford.
Kobayasi Y. 1952 – On the genus *Favolaschia* and *Campanella* from Japan. Journal of the Hattori Botanical Laboratory 8, 1–4.
Kong F, Tang L, He H, Yang FX et al. 2021 – Assessing the impact of climate change on the distribution of *Osmanthus fragrans* using Maxent. Environmental Science and Pollution Research 28, 34655–34663. Doi 10.1007/s11356-021-13121-3
Kornerup A, Wanscher JH. 1978 – Methuen handbook of color. 3rd Ed. E. Methuen and Co., Ltd., London, 252 p.
Li TH, Zhang WM, Song B, Shen TH, He Q. 1998 – Introduction to the Hainan Agarics. Journal of Jilin Agricultural University 20.
Li YC, Li MY, Li C, Liu ZZ. 2020 – Optimized Maxent model predictions of climate change impacts on the suitable distribution of *Cunninghamia lanceolata* in China. Forests 11, 302. Doi 10.3390/f11030302
Liu LN. 2020 – Taxonomy and molecular phylogeny of Mycenaceae in China. Doctoral dissertation, Jilin Agricultural University.
Liu PG, Yang ZL. 1994 – Studies of classification and geographic distribution on *Laschia* complex from the southern and southeastern Yunnan, China. Acta Botanica Yunnanica 16, 47–52.
Lobo JM, Jiménez-Valverde A, Real R. 2008 – AUC: a misleading measure of the performance of predictive distribution models. Global Ecology and Biogeography 17, 145–151.
Magnago AC, Trierveiler-Pereira L, Neves MA. 2013 – Contributions towards the knowledge of *Favolaschia* (Mycenaceae, Agaricomycetes) from Brazil. Mycosphere 4, 1071–1078. Doi 10.5943/mycosphere/4/6/5
Ortega-Huerta MA, Peterson AT. 2008 – Modeling ecological niches and predicting geographic distributions: a test of six presence-only methods. Revista Mexicana de Biodiversidad 79, 205–216.
Page RDM. 1996 – TreeView: application to display phylogenetic trees on personal computers. Bioinformatics 12, 357–358. Doi 10.1093/bioinformatics/12.4.357

Parmasto E. 1999 – *Favolaschia pegleri*, sp. nov. (Hymenomycetes). Kew Bulletin 54, 783–788. Doi 10.2307/4110876
Patouillard N. 1887 – Etude sur le genre Laschia Fr. Journal de Botanique 1, 225–231.
Patouillard N. 1900 – Essai Taxonomique sur les Families et les Genres des Hyménomycètes; Lucien Declume: Lons-le-Saaunier, France. Doi 10.5962/bhl.title.40287
Patouillard NT, Lagerheim G. 1892 – Champignons de l'Équateur. Pugillus II. Bulletin de la Société Mycologique de France 8, 113–140.
Pearce J, Ferrier S. 2000 – An evaluation of alternative algorithms for fitting species distribution models using logistic regression. Ecological Modelling 128, 127–147. Doi 10.1016/S0304-3800(99)00227-6
Pearson RG. 2007 – Species' distribution modeling for conservation educators and practitioners. American Museum of Natural History.
Peterson AT, Papes M, Eaton M. 2007 – Transferability and model evaluation in ecological niche modelling: a comparison of GARP and Maxent. Ecography 30, 550–560. Doi 10.1111/j.0906-7590.2007.05102.x
Phillips SJ, Miroslav D, Schapire RE. 2004 – Maxent software for species distribution modeling. Ecological Modelling 190, 231–259. Doi 10.1016/j.ecolmodel.2005.03.026
Posada D, Crandall KA. 1998 – Modeltest: testing the model of DNA substitution. Bioinformatics 14, 817–818. Doi 10.1093/bioinformatics/14.9.817
Ree RH, Smith SA. 2008 – Maximum likelihood inference of geographic range evolution by dispersal, local extinction, and cladogenesis. Systematic Biology 57, 4–14. Doi 10.1080/10635150701883881
Rehner SA, Buckley E. 2005 – A Beauveria phylogeny inferred from nuclear ITS and EF1-α sequences: evidence for cryptic diversification and links to Cordyceps teleomorphs. Mycologia 97, 84–98. Doi 10.3852/mycologia.97.1.84
Ronquist F, Huelsenbeck JP. 2003 – MrBayes 3: Bayesian phylogenetic inference under mixed models. Bioinformatics 19, 1572–1574. Doi 10.1093/bioinformatics/btg180
Shcheglovitova M, Anderson RP. 2013 – Estimating optimal complexity for ecological niche models: a jackknife approach for species with small sample sizes. Ecological Modelling 269, 9–17. Doi 10.1016/j.ecolmodel.2013.08.011
Singer R. 1945 – The *Laschia*-complex (Basidiomycetes). Lloydia 8, 170–230.
Singer R. 1974 – A monograph of *Favolaschia*. Beihefte zur Nova Hedwigia 50, 1–108.
Skrede I, Engh I, Binder M, Carlsen T et al. 2011 – Evolutionary history of Serpulaceae (Basidiomycota): molecular phylogeny, historical biogeography and evidence for a single transition of nutritional mode. BMC Evolutionary Biology 11, 1–13. Doi 10.1186/1471-2148-11-230
Smith SY, Currah RS, Stockey RA. 2004 – Cretaceous and Eocene poroid hymenophores from Vancouver Island, British Columbia. Mycologia 96, 180–186. Doi 10.1080/15572536.2005.11833010
Song J, Cui BK. 2017 – Phylogeny, divergence time and historical biogeography of *Laetiporus* (Basidiomycota, Polyporales). BMC Evolutionary Biology 1–12. Doi 10.1186/s12862-017-0948-5
Stamatakis A. 2006 – RAxML-VI-HPC: maximum likelihood-based phylogenetic analyses with thousands of taxa and mixed models. Bioinformatics 22, 2688–2690. Doi 10.1093/bioinformatics/btl446
Sunil K, Thomas JS. 2009 – Maxent modeling for predicting suitable habitat for threatened and endangered tree *Canacomyrica monticola* in New Caledonia. Journal of Ecology and the Natural Environment 1, 94–98.
Taylor TN, Hass H, Kerp H. 1999 – The oldest fossil ascomycetes. Nature 399, 648–648. Doi 10.1038/21349

Taylor TN, Hass H, Kerp H, Krings M, Hanlin RT. 2005 – Perithecial ascomycetes from the 400-million-year-old Rhynie chert: an example of ancestral polymorphism. Mycologia 97, 269–285. Doi 10.1080/15572536.2006.11832862

Thompson JD, Gibson TJ, Plewniak F, Jeanmougin F, Higgins DG. 1997 – The CLUSTAL X windows interface: flexible strategies for multiple sequence alignment aided by quality analysis tools. Nucleic Acids Research 25, 4876–4882. Doi 10.1093/nar/25.24.4876

Vilgalys R, Hester M. 1990 – Rapid genetic identification and mapping of enzymatically amplified ribosomal DNA from several *Cryptococcus* species. Journal of Bacteriology 172, 4238–4246. Doi 10.1128/jb.172.8.4238-4246.1990

Vizzini A, Zotti M. 2002 – *Favolaschia calocera*, a tropical species collected in Italy. Mycotaxon 82, 169–176.

Vizzini A, Zotti M, Mello A. 2009 – Alien fungal species distribution: The study case of *Favolaschia calocera*. Biological Invasions 11, 417–429. Doi 10.1007/s10530-008-9259-5

Walther GR, Post E, Convey P, Menzel A et al. 2002 – Ecological responses to recent climate change. Nature 416, 389–395. Doi 10.1038/416389a

White TJ, Bruns T, Lee S, Taylor J. 1990 – "Amplification and direct sequencing of fungal ribosomal RNA genes for phylogenetics," in *PCR Protocols: A Guide to Methods and Applications*, Innis MA, Gelfand DH, Sninsky JJ and White TJ (eds), New York, NY: Academic Press, 315–322. Doi 10.1016/B978-0-12-372180-8.50042-1

Wisz MS, Hijmans RJ, Li J, Peterson AT et al. 2008 – Effects of sample size on the performance of species distribution models. Diversity and Distributions14, 763–773.

Wu F, Li SJ, Dong CH, Dai YC, Papp V. 2020 – The Genus *Pachyma* (Syn. *Wolfiporia*) reinstated and species clarification of the cultivated medicinal mushroom "Fuling" in China. Frontiers in Microbiology 11, 590788. Doi 10.3389/fmicb.2020.590788

Wu F, Zhou LW, Vlasák J, Dai YC. 2022 – Global diversity and systematics of Hymenochaetaceae with poroid hymenophore. Fungal Diversity 113, 1–192. Doi 10.1007/s13225-021-00496-4

Yang KM. 2013 – Chinese Osmanthus. China Forestry Publishing, Beijing.

Yang XQ, Kushwaha SPS, Saran S, Xu JC, Roy PS. 2013 – Maxent modeling for predicting the potential distribution of medicinal plant, Justicia adhatoda L. in Lesser Himalayan foothills. Ecological Engineering 51, 83–87. Doi 10.1016/j.ecoleng.2012.12.004

Yang ZL. 2005 – Diversity and biogeography of higher fungi in China. In: Xu JP (ed) Evolutionary genetics of fungi. Horizon Bioscience, Norfolk, pp. 35–62.

Yi YJ, Cheng X, Yang ZF, Zhang SH. 2016 – Maxent modeling for predicting the potential distribution of endangered medicinal plant (*H. riparia* Lour) in Yunnan, China. Ecological Engineering 92, 260–269.

Yosio K. 1952 – On the genus *Favolaschia* and *Campanella* from Japan. The Journal of the Hattori Botanical Laboratory 8, 1–4.

Yu Y, Blair C, He X. 2020 – RASP 4: ancestral state reconstruction tool for multiple genes and characters. Molecular Biology and Evolution 37, 604–606. Doi 10.1093/molbev/msz257

Yu Y, Harris AJ, Blair C, He X. 2015 – RASP (Reconstruct Ancestral State in Phylogenies): a tool for historical biogeography. Molecular Phylogenetics and Evolution 87, 46–49. Doi 10.1016/j.ympev.2015.03.008

Yuan HS, Wei YL, Wang XG. 2015 – Maxent modeling for predicting the potential distribution of *Sanghuang*, an important group of medicinal fungi in China. Fungal Ecology 17, 140–145. Doi 10.1016/j.funeco.2015.06.001

Zhang LX, Chen XL, Xin XG. 2019 – Short commentary on CMIP6 scenario model intercomparison project (ScenarioMIP). Climate Change Research 15, 519−525.

Zhang QY, Dai YC. 2021 – Taxonomy and phylogeny of the *Favolaschia calocera* complex (Mycenaceae) with descriptions of four new species. Forests 12, 1397. Doi 10.3390/f12101397

Zhang Y, Tang JS, Ren G, Zhao KX, Wang XF. 2021 – Global potential distribution prediction of *Xanthium italicum* based on Maxent model. Scientific Reports 11, 16545. Doi 10.1038/s41598-021-96041-z

Zhu L, Song J, Zhou JL, Si J, Cui BK. 2019 – Species diversity, phylogeny, divergence time, and biogeography of the genus *Sanghuangporus* (Basidiomycota). Frontiers in Microbiology 10, 812. Doi 10.3389/fmicb.2019.00812